Compensation of the effect of humidity on dielectric strength of air insulation

NILANSHU MAHANT

DEPARTMENT OF ELECTRICAL ENGINEERING

CHALMERS UNIVERSITY OF TECHNOLOGY

Gothenburg, Sweden 2023

www.chalmers.se

Master's thesis 2023

Compensation of the effect of humidity on dielectric strength of air insulation

NILANSHU MAHANT

CHALMERS
UNIVERSITY OF TECHNOLOGY

Department of Electrical Engineering
Division of Electric Power Engineering
Chalmers University of Technology
Gothenburg, Sweden 2023

Compensation of the effect of humidity on dielectric strength of air insulation
NILANSHU MAHANT

Supervisor: Sr. Prin. Eng. Liliana Arevalo, Hitachi Energy
Examiner: Prof. Yuriy Serdyuk, Chalmers University of Technology

Master's Thesis 2023
Department of Electrical Engineering
Division of Electric Power Engineering
Chalmers University of Technology
SE-412 96 Gothenburg
Telephone +46 31 772 1000

Cover: Breakdown between the rod-plane electrode in air

Typeset in LaTeX
Gothenburg, Sweden 2023

Compensation of the effect of humidity on dielectric strength of air insulation

NILANSHU MAHANT
Department of Electrical Engineering
Chalmers University of Technology

Abstract

The effect of atmospheric conditions on the dielectric strength of air insulation is a complex issue that has been studied extensively around the world for many years. Although a lot of data is available, we are still a long way from full understanding of the impact of meteorological circumstances on the performance of air insulation. The purpose of this master's thesis is to investigate and to develop a new strategy for rectification of the atmospheric condition correction method suggested in the IEC-60060 standard. The current IEC technique leads to uncertainties in evaluations of withstand test results, in particular, significant deviations of insulation breakdown voltages at lower humidity conditions compared with standard atmospheric conditions. In order to account for the impact of low humidity on air insulation, data from earlier studies have been used. The effectiveness of environmental parameters has been studied using machine learning tools and regression analysis. As the result, equations for calculating the humidity correction factor are suggested. It is shown that the proposed method provides more accurate estimations compared with the standard correction procedure.

Keywords: HVDC, Insulation, Atmospheric condition, Low humidity, Air insulation, Rod-plane, Toroid-plane, Sphere-plane

Acknowledgements

Firstly, I would like to express my gratitude to my supervisors Liliana Arevalo, Yuriy Serdyuk, and Oscar Diaz for their unwavering support, feedback, valuable talks, direction, and inspiration in completing the project. I would like to express my gratitude to my examiner, Yuriy Serdyuk, for his assistance. I also want to thank Manne Segerlund in assisting and improving my skills during this project work. He had put a good effort to make this happen. At last, I would also like to thank my manager Pankaj Roy and all the other colleague from Hitachi energy for their assistance, directions, and recommendations during the project work.

Nilanshu Mahant, Gothenburg, 05-2023

List of Acronyms

Below is the list of acronyms that have been used throughout this thesis listed in alphabetical order:

HVAC	High Voltage Alternating Current
HVDC	High Voltage Direct Current
H.V.	High voltage
RMSE	Root Mean Square Error

Nomenclature

Below is the nomenclature of parameters that have been used throughout this thesis.

Parameters

H	Humidity	g/m^3
h_0	Absolute humidity	g/m^3
R	Relative humidity	%
t	Atmospheric Temperature	$°C$
t_0	Ambient Temperature	$°C$
P	Atmospheric Pressure	$mbar$
P_0	Absolute Pressure	$mbar$
E_{max}	Maximum Electric Field	kV
E_{mean}	Average Electric Field	kV
U_{50}	Breakdown Voltage/ Disruptive Discharge Voltage	kV
L	Minimum Discharge Path	m
δ	Relative Air Density	
E_{s0}	Electric field gradient for positive steamer propagation	kV
R^2	Coefficient of Determination	%

Contents

List of Acronyms **ix**

Nomenclature **xi**

List of Figures **xv**

List of Tables **xvii**

1 Introduction **1**
1.1 Introduction of HVDC 1
1.2 IEC 60060-1 1
1.2.1 Dielectric strength at lower humidity 2
1.3 Background 3
1.3.1 Atmospheric Correction 4

2 Theory **5**
2.1 What is machine Learning? 5
2.1.1 How to interpret fit function 6
2.1.1.1 What is model fitting? 6
2.1.1.2 Why is model fitting important? 7
2.1.1.2.1 Overfitting 7
2.1.1.2.2 Underfitting 8
2.1.2 Evaluation of the fitting tool 8
2.1.2.1 Other Fit Model 9

3 Methods **11**
3.1 IEC 60060 method 11
3.2 Experimental Set-up 15
3.2.1 Test Objects 16
3.2.2 New propose methods 17
3.2.3 Experimental data U_{50}/U_{50_0} 17

3.2.4 Method A 18
3.2.5 Method B 19
3.2.6 Method C 20
3.2.7 DC test 21
3.2.8 Switching Impulse Test 25

4 Results **27**
4.1 DC Results 27
4.1.1 Rod-Plane 28
4.1.2 Toroid 320-Plane 29
4.1.3 Toroid 600-Plane 31
4.1.4 Sphere 250-Plane 32
4.2 Impulse test 35
4.2.1 Rod-Plane 36
4.2.2 Toroid-plane 38
4.2.3 Sphere-Plane 40

5 Conclusion **43**
5.0.1 Limitation 44

Bibliography **45**

List of Figures

2.1 Machine learning regression analysis flowchart 5
2.2 Machine learning overfitting of data 7
2.3 Machine learning underfitting of data 8

3.1 g vs. m and w values 13
3.2 Absolute humidity of air as a function of dry and wet-bulb thermometer readings 14
3.3 Flowchart for current IEC method 15

4.1 Rod-plane gap distance 1 m 28
4.2 Toroid 320-plane gap distance 0.5 m 29
4.3 Toroid 320-plane gap distance 0.75 m 29
4.4 Toroid 320-plane gap distance 1 m 30
4.5 Toroid 600-plane gap distance 0.75 m 31
4.6 Toroid 600-plane gap distance 1 m 31
4.7 Sphere 250-plane gap distance 0.5 m 32
4.8 Sphere 250-plane gap distance 0.75 m 33
4.9 Sphere 250-plane gap distance 1 m 33
4.10 Sphere 250-plane gap distance 1 m 2 34
4.11 Rod-Plane gap distance 0.6 m 36
4.12 Rod-Plane gap distance 1 m 36
4.13 Rod-Plane gap distance 2 m 37
4.14 Toroid 350-Plane gap distance 0.6 m 38
4.15 Toroid 425-Plane gap distance 0.6 m 38
4.16 Toroid 600-Plane gap distance 1 m 39
4.17 Toroid 600-Plane gap distance 2 m 39
4.18 Sphere 150-Plane gap distance 0.6 m 40
4.19 Sphere 500-Plane gap distance 1 m 41
4.20 Sphere 500-Plane gap distance 2 m 41

List of Tables

2.1 DC final equation as per the geometry and humidity condition 10

3.1 m and w exponents values depends in g 12
3.2 DC proposed method B eq.'s as per geometry 19
3.3 Method C 20
3.4 DC test Rod-plane 21
3.5 DC test Toroid 320/60-plane gap distance 0.5 meter 22
3.6 DC test Toroid 320/60-plane gap distance 0.75 meter 22
3.7 DC test Toroid 320/60-plane gap distance 1 meter 22
3.8 DC test Toroid 320/60-plane gap distance 1 meter 2 23
3.9 DC test Toroid 600/100-plane gap distance 0.75 meter 23
3.10 DC test Toroid 600/100-plane gap distance 1 meter 23
3.11 DC test Sphere 250-plane gap distance 0.5 meter 24
3.12 DC test Sphere 250-plane gap distance 0.75 meter 24
3.13 DC test Sphere 250-plane gap distance 1 meter 24
3.14 DC test Sphere 250-plane gap distance 1 meter 2 25
3.15 Switching impulse Rod-plane gap 0.5 meter 25
3.16 Switching impulse test Rod-plane gap 1 meter 25
3.17 Switching impulse test Rod-plane gap 2 meter 25
3.18 Switching impulse test Sphere 150-plane gap 0.6 meter 26
3.19 Switching impulse test Toroid 350-plane gap 0.6 meter 26
3.20 Switching impulse test Toroid 425-plane gap 0.6 meter 26
3.21 Switching impulse test Toroid 600-plane gap 1 meter 26
3.22 Switching impulse test Toroid 600-plane gap 2 meter 26

4.1 DC equations as per the geometry and humidity condition 28
4.2 SI equations as per the geometry 35

1

Introduction

1.1 Introduction of HVDC

Power demands are increasing dramatically around the world in order to attain the goal of a sustainable future this increases power demand in transmission, distribution, and consumption. To meet demand, HVDC will play a key role in the world in the future. When compared to HVAC, this system has various advantages. As a result, high-voltage direct-current (HVDC) systems are increasingly being used in transmission systems. It has significant advantages, including the ability to integrate renewable resources, bulk power transmission across long distances, lower long-distance costs, fewer losses when compared to high-voltage alternating current (HVAC), and flexible grid operation. The high-voltage direct current (HVDC) system is utilized for high-power long transmission and plays an important role in the power system. As a result, the HVDC system's ability to operate more reliably in the power system. When power system insulation fails, the dependability of the power system is jeopardized. This failure is caused by two major factors: internal and external overvoltage. Internal overvoltage can develop as a result of switching operation, short circuits, ground-to-phase faults, resonance, and other factors [41] and external overvoltage is common during the lightning stroke. This introduces traveling waves into the system, resulting in overvoltage in the power system [41]. This could be the cause of a breakdown in the power system.

1.2 IEC 60060-1

However, various environmental factors such as temperature, pressure, and humidity have an effect on High Voltage electrical equipment, producing failure of transmitting the power during real-world deployment of high voltage equipment. It is incorporated into the design solution supplied by IEC-60060 as a correction factor *(k)* that must be addressed during the design process under varied atmospheric conditions to reduce inaccuracy. For converting the observed voltage or test voltage from non-

standard to standard reference environment or vice versa, an IEC-recommended correction process is usually utilized. This k factor however, deviates when the temperature is low and the humidity is exceedingly low [1]. To verify the accuracy of the current IEC 60060 data, reference data from the rod-plane, sphere-plane, and toroid-plane are used. After applying the IEC 60060 correction technique to this data, the corrected breakdown voltage is then obtained. Then this corrected breakdown voltage is compared with standard atmospheric condition breakdown voltage. In the case of an indoor high-voltage installation, the shape of the electrode is frequently adjusted to achieve more compact design than in the case of a rod-plane gap. As a result, it is critical to confirm the accuracy of the recommended correction in these circumstances. The results of the paper [2] [3] [4] are reported in this study for varied uniformity and air gaps. These data were then adjusted to match the IEC 60060 standard reference correction. In this study the experimental data available only for the dc and switching impulse test and there is no availability of ac test data. So, the proposed method in this paper is only for the dc and switching impulse test.

The main focus of this study is on determining the inaccuracy in the IEC 60060 atmospheric correction method and offering an acceptable method with different geometry, gap distance, and voltage level. The new technology machine learning tool was utilized to find a critical parameter and regression analysis used to identify the mathematical expression in this study. To grasp the algorithm between two parameters, machine learning includes an inbuilt function which is considerably easier nowadays.

1.2.1 Dielectric strength at lower humidity

A number of factors can affect the dielectric strength of external insulation, including the type of overvoltage, stresses, shape, position, and ambient air [42]. The dielectric strength of air and how it affects outside insulation at very low humidity on direct current and switching impulse voltage are the major topics of this study. The primary goal of the study is to suggest a humidity correction factor (K factor) for different electrode layouts. The H/δ ratio is represented by the K value and H denotes absolute humidity, while δ is the relative air density of the material. There are two type of humidity H denotes absolute humidity and R is the relative humidity. Despite several studies by world-renowned academics, the effect of air density on electrode shape, gap spacing, and other parameters remains unknown. There are some discrepancies detected under various voltage situations when compared to IEC-60060.

1.3 Background

Air gaps are commonly used as insulation between conductors, rod-planes, sphere-planes, and overhead line towers. Air insulation is important in the design of an H.V. system. For the selection of air insulation between two high voltage equipment, the basic concept of electrical discharges/ formation of electron avalanche in air and the effect of atmospheric conditions on the air insulation required more understanding. The selection of air insulation depends on factors like amplitude of voltage, frequency, and type of voltage i.e. i) DC test, ii) Impulse test iii) AC test. The strength of air gaps affected by many factors like, humidity, pressure, temperature, gap distance and type of geometry. Due to this reason the electrical stress in insulation causes failure, which includes voltage collapse. This type of failure produces a permanent loss of strength in solids, but merely a transitory loss in liquids or gases. Flashover occurs when a discharge occurs in gas between two geometries/equipment's over a solid surface. It is referred to as the disruptive discharge voltage. The compensate effect of different atmospheric condition can aid in the finalization of the HVDC substation footprint based on actual site conditions.

The compensate effect of different atmospheric condition can aid in the finalization of the HV substation footprint based on actual site conditions. There are more authors that observed that atmospheric condition are reason for breakdown. However, the humidity variation had the greatest impact [3]. At varying humidity levels, electrons have varied bandwidths. This could have an impact on the how researchers understand about generation and growth of electron avalanches caused by electron impact in strong electric fields ionizing neutral atoms and molecules. Understanding the production of electric fields on different surfaces will result in a breakdown inside the actual site. As a result, the true problem will arise when HVDC equipment is designed in areas where humidity, pressure, and temperature levels vary greatly throughout the year. This could be the cause of the breakdown. IEC 60060-1 proposes an atmospheric correction and humidity correction method to estimate the corrected breakdown voltage. However, this strategy does not woel for all geometry because the IEC 60060-1 is generalized method for all the geometry as a result it has larger error in corrected breakdown voltage compare with standard atmospheric condition breakdown voltage. IEC 60060 method only works for rod-plane geometry [1] that's why many authors recommending to find new approach for other geometries.

1.3.1 Atmospheric Correction

Pressure and temperature are two elements that are included in the atmospheric correction. The pressure and temperature values fluctuate depending on altitude [22]. The pressure decreases at high altitude and breakdown voltage of external insulation is affected by the surrounding environment. An increase in either air density or humidity raises the breakdown voltage for a specific discharge path in air. When the relative humidity rises above 80%, the breakdown voltage becomes uneven [43]. The atmospheric correction factor k_t varies depending on the air density correction factor k_1 and humidity correction factor k_2. Correction factors must be applied to adjust the actual atmospheric condition to the standard reference atmospheric condition.

2

Theory

2.1 What is machine Learning?

In simple words, machine learning is a type of artificial intelligence (AI) that allows software applications to become more accurate at predicting outcomes without being explicitly programmed to do so. Machine learning algorithms use previous data to predict the future and create a function based on that predicting value [22]. It is much easier to grasp the algorithm between the different coordinates when using the machine learning program within MATLAB. Machine learning makes it easier and provides a 95% confidence interval. This internal data is obtained using the various fitting function tools accessible in the MATLAB application. For this master's thesis, the MATLAB machine learning regression learner application was used to predict the k values and $U_{50corrected}$ values using machine learning technologies.

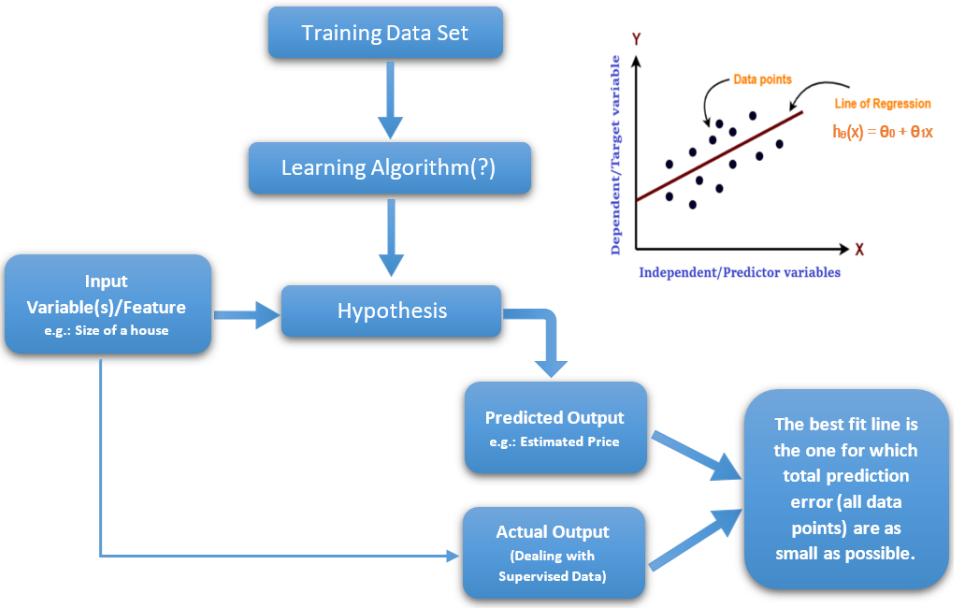

Figure 2.1: Machine learning regression analysis flowchart

Figure 2.1 represents the flowchart of the machine learning technique. It is manda-

tory to divide the data into train and test data. This is done randomly by MATLAB. It has an inbuilt function to select the data randomly for train and test data. The data selected for the train and test are 80% and 20% respectively. These features will give a hypothesis that will tell the algorithm between the data. This hypothesis will predict the output data with error compared with the actual value. The best fit line will tell the error between the actual data and the predicted value.

2.1.1 How to interpret fit function

The Fit function in MATLAB is used to train the data values in order to attain higher accuracy. The Fit function modifies weights based on data values to obtain greater accuracy. The process of fitting models to data and analyzing the fit accuracy is known as data fitting. It is used in this application to learn about mathematical equations and nonparametric approaches. The best fitting option to available data-sets is easy to understand when using the fit function with different data-sets. This fitting function indicates that if the fit to the data is not accurate, the results it provides will not be accurate enough for practical decision-making.

2.1.1.1 What is model fitting?

Model fitting assesses how effectively a machine learning model generalizes to data that is comparable to that on which it was trained. A well-fitted model yields more accurate results. An overfitted model closely matches the data. An underfitted model does not match closely enough.

Each machine learning algorithm has a set of basic parameters that can be modified to improve its accuracy. During the fitting process, run an algorithm on data for which the target variable is known, often known as "labeled" data, to generate a machine learning model. The results should then be compared to actual, observed values of the target variable to determine their correctness. Then, using that knowledge, tweak the algorithm's standard settings to lower the level of inaccuracy, making it more accurate in detecting patterns and relationships between the rest of its features and the target. This approach needs to be repeated until the algorithm discovers the best settings for producing legitimate, practical, and usable for the real word application.

2.1.1.2 Why is model fitting important?

The essence of machine learning is model fitting. If the model does not match the data appropriately, the results it provides will be insufficiently accurate to be useful for practical decision-making. Hyperparameters in a correctly fitted model capture the complicated interactions between known factors and the target variable, allowing it to identify useful insights or make accurate forecasts.

Fitting is an automatic method that ensures machine learning models have the particular parameters that are most suited to solving specific real-world problems with high accuracy.

2.1.1.2.1 Overfitting Occurs when a machine learning model becomes overly customized to the data on which it was trained and hence loses applicability to any other dataset. Overfitting occurs when a model is so particular to the original data that applying it to new data might result in problematic or erroneous outcomes, and thus less-than-optimal judgments [45] [46].

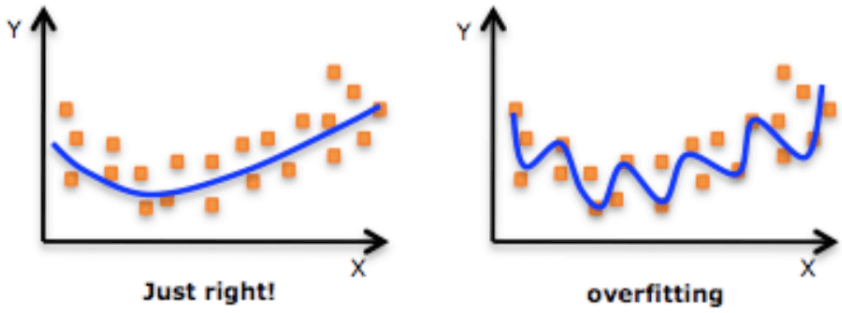

Figure 2.2: Machine learning overfitting of data

It is significant because of the Overfitting leads the model to misinterpret the data it learned from. An overfitted model will be less accurate on new, similar data than a more widely fitting model, but it will appear to be more accurate when applied to training data. With no overfitting protection, the model may need train and deploy a model that can be believed can be very accurate.

Using an overfitted model might lead to a slew of issues. For example, if the model is 95% accurate in predicting the value of input data. But in reality, it is overfitted and has an accuracy closer to 60%, applying it to other data. Then it can be

observed whether it's accurate or not. If the prediction value is not accurate it will misguide the system.

2.1.1.2.2 Underfitting It occurs when a machine learning model is not complex enough to accurately capture associations between characteristics in a dataset and a target variable. An underfitted model produces troublesome or erroneous results on new or untrained data, and it frequently performs badly even on training data.

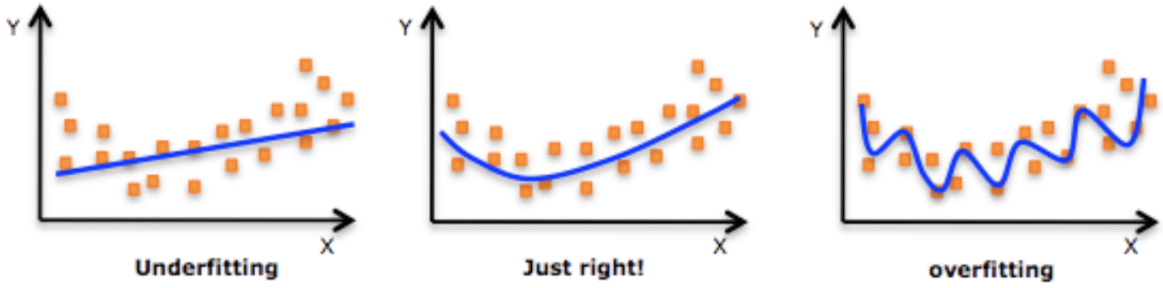

Figure 2.3: Machine learning underfitting of data

It is significant because adopting unsuitable models for decision-making can be costly for enterprises. For example, an underfitted model may suggest that spending more on marketing will always result in more sales while, in fact, the model fails to capture a saturation effect (at some point, sales will flatten out no matter how much more you spend on marketing). If a company relies on that methodology to decide its marketing budget, it must overspend on marketing.

2.1.2 Evaluation of the fitting tool

Several models were employed using input data in this thesis. The regression learner app within MATLAB already has a built-in model. This application includes 24 built-in models that provide the best fit model to the input data. The best fitting model is also determined by the input data, and there is only one output choice to choose from. The output is entirely dependent on the input data. If the input parameters are pressure, temperature, relative humidity, humidity, and disruptive discharge voltage, the prediction of the output voltage level is nearly the same to what the regression learner app entered. To obtain a correct output, the U_{50}/U_{500} is employed for the particular geometry. The inaccuracy of the disruptive discharge

voltage with this k value is quite minimal at low humidity conditions compared with standard humidity conditions. As a result, evaluating the value of k using U_{50}/U_{500} is more appropriate to the real results. So, utilizing the U_{50}/U_{500} will get the optimum equation for k with the help of the regression learner app and fit function.

This equation is evaluated by computing the RMSE (Root Mean Square Error). Also, in a regression model, the R^2 (Coefficient of determination) is a statistical metric that determines the proportion of variance in the dependent variable that can be explained by the independent variable. It is suggested that the values of RMSE and R^2 be closer to one. Consider the optimal model/equation for the input and output if the RMSE and R^2 values are near to 1 [44]. RMSE may be determined using 2.1, and R^2 can be calculated with 2.2.

$$RMSE = \sqrt{MSE} = \sqrt{\frac{1}{N}\sum_{i=1}^{N}\left(k_i - \hat{k}\right)^2} \tag{2.1}$$

$$R^2 = 1 - \frac{\sum\left(k_i - \hat{k}\right)^2}{\sum\left(k_i - \bar{k}\right)^2} \tag{2.2}$$

Whre, In Eq. 2.1 k_i represent the original values and $\hat{k}$ represents the anticipated value of k. As a result, the model can be evaluated using the eq. 2.1 - 2.2. If the RMSE value is less than one and the R^2 value is closer to 0, that model is considered the best model for the data.

2.1.2.1 Other Fit Model

During this master's thesis, the following input data for the regression learner app were observed: pressure, temperature, relative humidity, absolute humidity, and breakdown voltage. The regression learner app's best fitting model is Gaussian Process Regression Exponential GPR. However, the variable exists in the Gaussian equation. This variable consists of the mean and standard deviation. This variable's value changes depending on the input data. So, if the input data changes, the output of the Gaussian dynamic changes. This problem does not have in a polynomial or exponential solution. Polynomial, exponential, Fourier, gaussian, power, rational, and lsqcurvefit are among the possible fit functions [47]. Other fit functions are also employed in this thesis. However, the best match with the available data is a polynomial 2^{nd} order equation and an exponential equation it was observed by the regression analysis tool. The fitting function and corresponding equation are represented in table 2.1.

Table 2.1: DC final equation as per the geometry and humidity condition

MATLAB Fit function	
Fit type	**Equation**
Poly2	$\mathrm{ah}^2 + bh + c$
Poly3	$\mathrm{ah}^3 + bh^2 + ch + d$
Expo1	$\mathrm{a}*\mathrm{e}^{(bh)}$
Expo2	$\mathrm{a}*\mathrm{e}^{(bh)} + c * e^{(dh)}$
Gaussian	2.3
Power	$a^{(bh)}$

$$Gaussian = \frac{1}{\sigma\sqrt{2\pi}} e^{-\frac{(x-\mu)^2}{2\sigma^2}} \tag{2.3}$$

Where, μ = Mean
σ = Standard Deviation

The underlying issue with this approach is that it cannot be employed because it requires input data all of the time. Because the gaussian equation involves the mean value and standard deviation, it requires input data. As a result, the gaussian equation cannot be employed.

3

Methods

3.1 IEC 60060 method

This method uses an empirical method based on an experiment to determine the breakdown voltage obtained under static and direct test conditions at various distances, humidities, temperatures and pressure levels. The IEC 60060 [21] humidity correction factor are utilized to correct 50% breakdown voltage as well as withstand voltage. This correction method provides an improved breakdown voltage under actual humidity conditions compared to standard humidity conditions (11 g/m^3).

When it comes to switching impulse voltage with varying long air gaps, this strategy has proven to be acceptable. The following are the standard pressures, temperatures, and humidities:

Pressure: 1013 mbar
Temperature: 20 C
Humidity: 11 g/m^3

The atmospheric correction factors for the breakdown voltage are k_1 and k_2. Whereas, k_1 is the air density correction factor, and k_2 is the humidity correction factor:

$$k_{DC} = 1 + 0.014(\frac{h}{\delta} - 11) - 0.00022(\frac{h}{\delta} - 11)^2 \tag{3.1}$$

$$k_{AC} = 1 + 0.012(\frac{h}{\delta} - 11) \tag{3.2}$$

$$k_{Impulse} = 1 + 0.010(\frac{h}{\delta} - 11) \tag{3.3}$$

Eq. 3.1 to 3.3 are 3 different equation used for the different test voltage. In the above equations (3.1 to 3.3) the values k is directly propositional to the humidity and inversely propositional to the air density factor and figure.3.3 represents the whole IEC 60060 [21] method.

To determine the $U_{50_{corrected}}$ the value of g has been used. The value of g is a correlation between the breakdown voltage and steamer propagation which depends on the type of discharges, if the discharges are positive then the value of steamer propagation will be between 450 kV to 550 kV while for the negative steamer discharges the value of steamer propagation will be in between 750 kV to 1000 kV. The value of g also depends on the discharge path and the air density factor as well as humidity correction parameter value k. Eq. 3.4 represents the value of g. The m and w are the exponents of air density correction and humidity correction respectively, which are dependent on the value of g. These exponents are introduced to determine the correction factor table 3.1 represents the values of m and w in relation to g.

$$g = \frac{U_{50}}{500 L \delta k} \tag{3.4}$$

Table 3.1: m and w exponents values depends in g

$\boldsymbol{g}$	$\boldsymbol{m}$	$\boldsymbol{w}$
< 0.2	0	0
0.2 to 1	$g(g-0.2)/0.8$	$g(g-0.2)/0.8$
1 to 1.2	1	1
1.2 to 2	1	$(2.2-g)(2-g)/0.8$
> 2	1	0

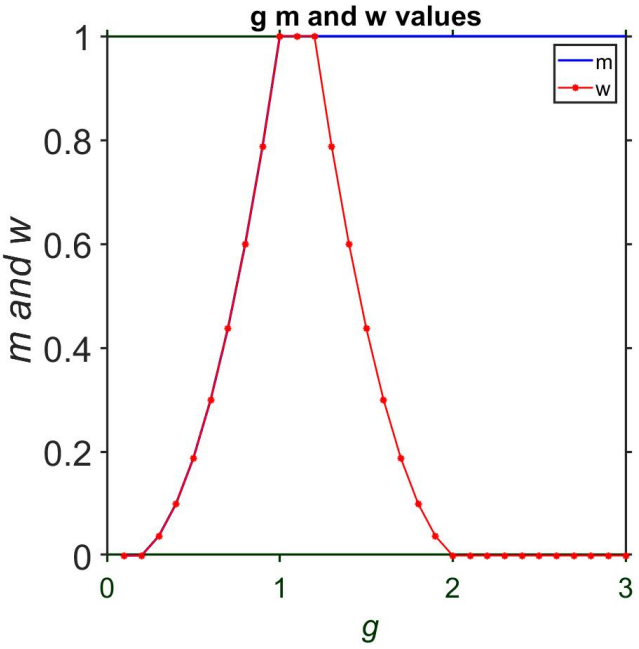

Figure 3.1: g vs. m and w values

Humidity can be calculated by measuring the relative humidity and temperature. Absolute humidity is calculated by following eq. 3.5. This measurement can also be done by means of ventilated wet and dry bulb hygrometer. The absolute humidity as a function of the thermometer reading is determined from 3.2, it is also possible to calculate relative humidity. It is critical to supply appropriate airflow to achieve a steady condition and to properly read the thermometers to avoid significant inaccuracies in humidity measurement.

$$h = \frac{6.11 \times R \times e^{\frac{17.6 \times t}{243+t}}}{0.4615 \times (273 + t)} \tag{3.5}$$

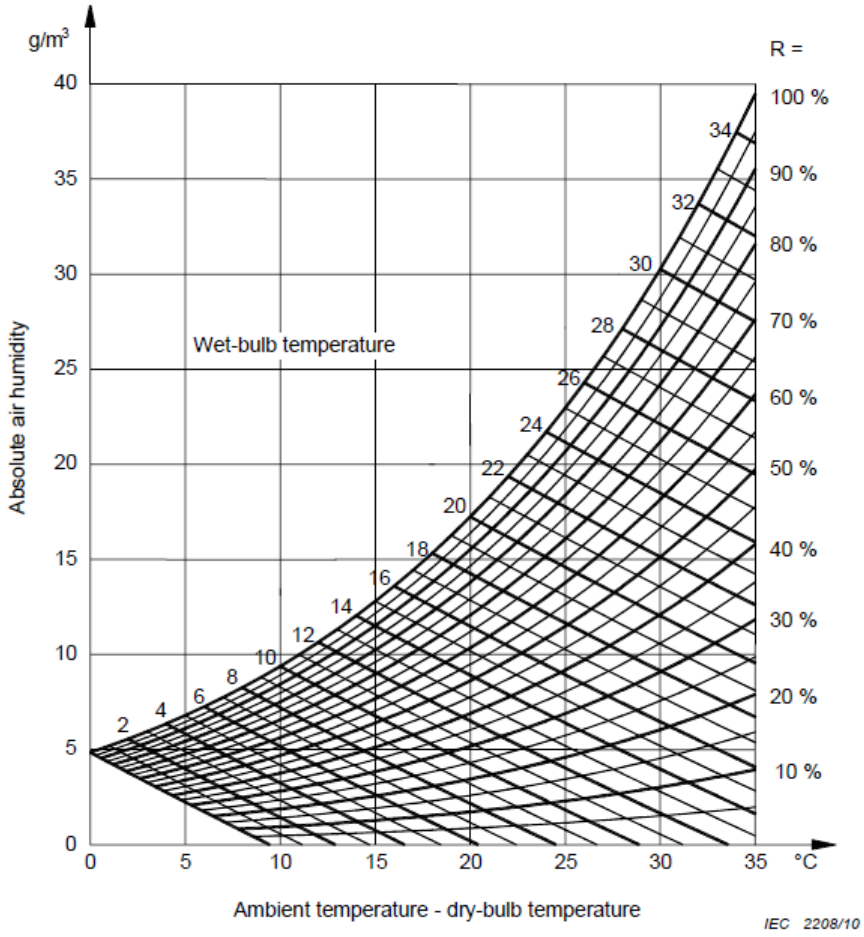

Figure 3.2: Absolute humidity of air as a function of dry and wet-bulb thermometer readings

The total correction factor depends on the atmospheric correction factor and humidity correction factor [21], which are calculated by the following eq.'s 3.6 3.7. So, the total correction factor represents in eq. 3.8

$$k_1 = \delta^m \tag{3.6}$$

$$k_2 = k^w \tag{3.7}$$

$$k_t = k_1 \times k_2 \tag{3.8}$$

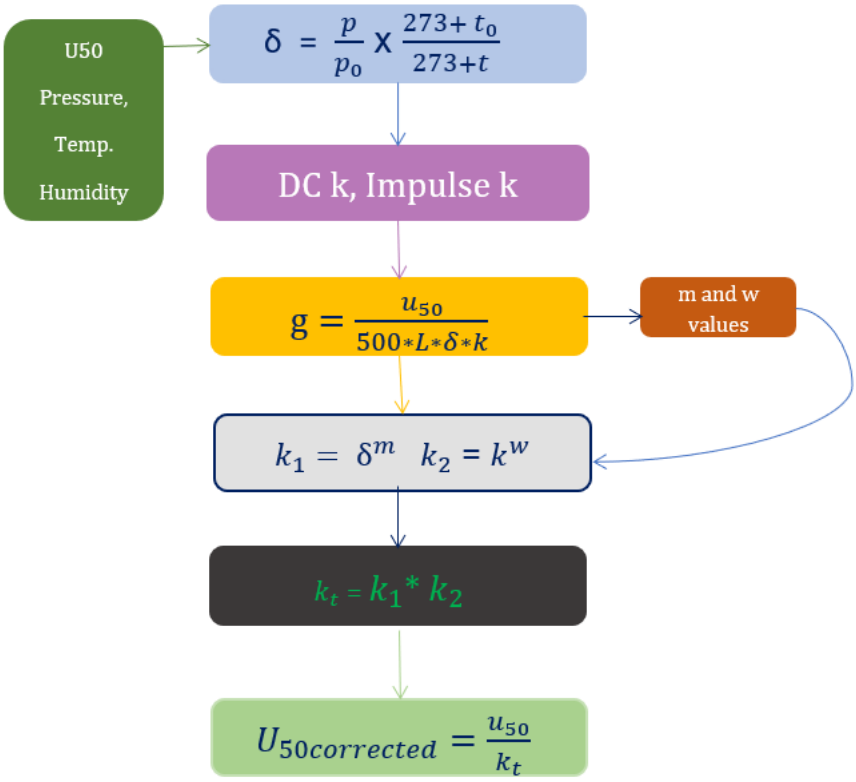

Figure 3.3: Flowchart for current IEC method

Figure. 3.3 represents the current IEC-60060-1 method flowcharts. Where, parameters in flowchart are pressure P ($mbar$), Temperature T C, Absolute Humidity H (g/m^3) , gap distance d (m), Breakdown voltage u_{50} (kV), IEC Corrected breakdown voltage $U_{50_{corrected}}$.

The IEC correction method was applied to collected data from Hitachi energy [2] [3] [4]. The IEC approach yields a substantially greater corrective breakdown voltage than the measure breakdown voltage. The discrepancy is at lower humidity levels, where the difference between the measured and adjusted values is approximately 24 % [1].

3.2 Experimental Set-up

In order to study the breakdown voltage at different atmospheric conditions, test for different electrode arrangements under different stresses type switching impulse

and DC were studied in [2] [3] [4]. The experimental data acquired from the Hitachi energy test campaign at STRI, Sweden, is presented in this publication. This data set contains two records: switching impulse voltage and DC test voltage. To find out how pressure, temperature, and humidity affect different geometries and gap distances, tests were conducted at various pressures and temperatures. The test was run using both uniform and non-uniform geometry under a different range of humidity conditions. All testing was carried out indoors in a high voltage hall with adjustable humidity, pressure, and temperature. Through a window in the chamber, a video camera was utilized to inspect and record the test. After the air temperature and humidity in the chamber had been regulated and recorded, the test voltage level was applied. The humidity and air temperature of the chamber were also recorded after each test. Because attaining the various atmospheric conditions took a lengthy time, as result all tests was performed under near-standard atmospheric circumstances and varying humidity conditions, as shown in sectionTest Results. The uniformity factor $\eta = E_{max}/E_{mean}$ estimates the electric field homogeneity of the setups.

The voltage level of the 50% breakdown probability U_{50} for uniform and non-uniform switching impulse tests was derived using the well-known up-and-down approach. The tests were carried out using a conventional 250/2500 μs positive switching impulse. A total of 30 distinct switching impulses were used, with a breakdown probability of 50%.

The average breakdown voltage level for the DC voltage test was calculated using the results of the 10 average breakdown voltage tests. The test was carried out with a positive DC voltage. The applied voltage to the system begins at 75% of the projected breakdown voltage and the voltage level was continuously raised to 2% per second [3] followed by the approach recommended by IEC 60060.

3.2.1 Test Objects

Rod-plane, sphere-plane, and two different toroid-plane geometries were employed in the test. The DC voltage has been applied to rod-plane, two distinct toroid diameters 320 600 mm, and sphere diameter 250. The switching impulse test uses the following geometries: rod-plane, toroid diameters of 350 mm, 425 mm, 600 mm, and sphere diameters of 150 mm 500 mm. This toroid and sphere of varying sizes were tested with the plane at various air gaps [2] [3] and [4].

3.2.2 New propose methods

This publication has provided different methods for rectifying the current IEC 60060 method. The current IEC technique applies to rod-plane geometry and the rod-plane geometry has not been altered in this study. This proposed approach only works with toroid-plane and sphere-plane geometry. This approach was created with MATLAB software and It has several fitting functions. Because the data supplied for this study is limited, the methods shown in this section have not been validated for other geometries arrangements. The machine learning curve-fitting application provides several options for selecting input and output data. This tool is handy for understanding the relationship between the various factors.

3.2.3 Experimental data $\mathbf{U}_{50}/U_{50_0}$

This method was evaluated by the CIGRE 33 group [40]. This method differs from the existing IEC 60060 method in two ways. Eq.3.1 and eq. 3.3 are IEC 60060 equations to calculate the value of k for DC test and switching impulse test respectively. In this [40] approach the value of k was modified for the less % error. This method's drawback was that the standard breakdown voltage had to be known from the start, which limited its usefulness for general applications. According to the suggested methodology in current study, g values change with shifting voltage conditions as well as with the separation between the two geometries. The g values were subjected to the three conditions listed in eq no. 3.10 3.11 3.13.

$$k = \frac{U_{50}}{U_{50_0}} \tag{3.9}$$

The new propose g specify in 3 different method, which is mentioned in eq no. 3.10

$$g = \frac{U_{50}}{500L\delta k} \tag{3.10}$$

eq no. 3.10for condition $U_{50} < 300kV \quad L < 1m$

$$g = \frac{U_{50}}{550\delta k} \tag{3.11}$$

eq no.3.11 for condition $U_{50} > 300kV \quad L < 1m$

$$g = \frac{U_{50}}{550L\delta k} \tag{3.12}$$

eq no.3.13 for condition $U_{50} > 300kV \quad L > 1m$

Equation 3.10 to 3.13 are a contribution of this master thesis. The g value is subjected to three different situations. When the breakdown voltage level U_{50} is less than 300 kV and the gap distance between the two geometry is less than 1-meter then eq. 3.10 applies. Equation 3.11 applies when the breakdown voltage level is greater than 300 kV and the gap distance between two geometries is less than 1-meter. Equation 3.13 applies when the breakdown voltage level is greater than 300 kV and the gap distance is greater than 1 meter.

The correction method is based on a semi-spherical model and has a wider range of application and simplicity. It determines atmospheric correction factors using dimensionless parameters G_0. In eq 3.10, d represents the minimum discharge path in meters, and E_{s0} represents the electric gradient for positive streamer propagation under ordinary air circumstances. Whereas E_{s0} is assumed to be 500 kV/m and δ is the relative air density computed as follows:

$$\delta = \frac{P}{P_0} \times \frac{273 + t_0}{273 + t} \tag{3.13}$$

Method proposed by the CIGRE 33 group with changing in factor g is applicable to both the voltage, DC test and Switching Impulse test voltage.

3.2.4 Method A

The newly proposed approach A was tested using existing data sets and built using the latest machine learning techniques. Current MATLAB tool for machine learning application was used in this process. Machine learning was used to understand the interactions of the algorithm with different parameters. Using this new tool, the algorithm between various input data and output was easily understood. Then, regression analysis was used to find an equation. Thus the information was separated according to geometry. Whereas this tool was applied to the same geometry but with a different discharge path, such as a rod-plane with a discharge path of 0.6 m., 1 m., 2 m., and different fit functions were used in this method for different geometries and humidity conditions. Regression analysis provides the following equation to calculate the parameter k to estimate the humidity correction factor k_2.

$$k_{DC} = 1 - 0.005733 * (\frac{h}{\delta} - 11) - 0.002811 * (\frac{h}{\delta} - 11)^2 - 0.0001773(\frac{h}{\delta} - 11)^3 \quad (3.14)$$

$$k_{Impulse} = 0.9786 * \mathrm{EXP}\left(0.002509 * \left(\frac{\mathrm{h}}{\delta} - 11\right)\right) \quad (3.15)$$

Equation. 3.14 and 3.15 were applied to all geometry and the % error for the corrected breakdown voltage of actual atmospheric condition compare with the standard atmospheric condition and % lesser than the current IEC 60060 [21]. In the current IEC methodology, the polynomial's overall degree is 2, whereas in method A for the DC voltage test, it is 3. For the switching impulse test the exponential 1^{st} order function is the best fitting with all geometry and different discharge paths. In comparison to the IEC method, this methodology contains two alterations that can be used to compute the corrected breakdown voltage. This approach has two variations to calculate the corrected breakdown voltage compare with IEC method, the first variation in parameter k which is mentioned in eq. 3.14, 3.15 and the second variation are to calculate the value g with the condition of voltage and discharge path between two geometries.

3.2.5 Method B

In this method, data sets were divided based on geometry. The impact of current humidity correction variables is investigated using four different geometry data sets in this study. Using the MATLAB software, Method B was applied to available geometries to determine the correlation between input and output. It was only used on DC test data due to the larger error (when used to switching impulse tests) when compared to Method A and IEC 60060 [21]. For the best fitting tool, the same geometry was used with multiple discharge paths and humidity conditions in this method. Four distinct geometry equations have been developed. Which are listed in the table below:

Table 3.2: DC proposed method B eq.'s as per geometry

DC proposed method B eq.'s as per geometry	
Geometry	**Eq.'s to calculate k parameter**
Rod-plane	$-0.5639 * (\frac{h}{\delta} - 11)^2 + 16.71 * (\frac{h}{\delta} - 11) + 462.3$
Toroid 320-plane	$0.9251 * (e^{0.006838(\frac{h}{\delta} - 11)})$
Toroid 600-plane	$1.11 * (e^{-0.000785(\frac{h}{\delta} - 11)})$
Sphere-plane 250	$0.9735 * (e^{0.002571(\frac{h}{\delta} - 11)}) + 0.1886 * (e^{-4.24(\frac{h}{\delta} - 11)})$

Table 3.2 represents the equations of the method B. The geometry column represents the geometry configuration used in this method and right side shows the best fitting equation for that particular geometry.

3.2.6 Method C

This method is completely different from the other methods as no pre-discharge is involved for the calculation of the correction factor k_t. Other correction methods such as IEC 60060, Experimental data U_{50}/U_{50_0}, Method A, and Method B consider the correlation of the breakdown voltage with the steamer propagation process to calculate the corrected breakdown voltage whereas it has not been used in method C. As a result exponents m and w were not calculates in method C. i.e.entire steamer propagation correlation between breakdown voltage and steamer propagation has been removed in method C. Method C has been only applied to DC type test data due to the high % error in the switching impulse test.In order to determine the corrected breakdown voltage, Method C is divided into two sections: geometry and humidity (<3 $g/m3$ and >3 $g/m3$). The equation presented in Table 3.3 separates as per above two sections. Additionally, the air density component was not taken into account while calculating $U_{50_{Corrected}}$.

Table 3.3: Method C

DC comparison of IEC and proposed method		
Geometry	**Gap (m)**	**Eq.'s to calculate k parameter**
Toroid-plane 320	<3	$-0.00483 * h^2 + 0.018 * h + 0.9653$
Toroid-plane 320	>3	$0.001 * h^2 - 0.0008 * h + 0.9519$
Toroid-plane 600	<3	$1 * (e^{-0.00054 * h})$
Toroid-plane 600	>3	$1 * (e^{-0.00054 * h})$
Sphere-plane 250	<3	$0.93 * (e^{-0.0009 * h})$
Sphere-plane 250	>3	$0.91 * (e^{0.0084 * h})$

Table 3.3 represents the geometry with varying humidity conditions. It was already mentioned from the beginning that, the behavior of breakdown voltage was changing at extreme low humidity which was observed at humidity level $3g/m^3$. As a result, technique C is divided into <two sections: low humidity $<3g/m^3$ and high humidity conditions $>3g/m^3$.

3.2.7 DC test

Table 3.4 to 3.14 represents the DC test input data and output with respect to different methods showed in the method section. Table 3.15 to 3.22 represents the switching impulse test. Where H denotes the absolute humidity in g/m^3, U_{50} denotes experimental breakdown voltage in [kV], IEC represents the corrected breakdown voltage of IEC 60060 method, %IEC represents the error between standard atmospheric condition breakdown voltage and actual atmospheric condition breakdown voltage in %, U_{50}/U_{50_0} represents the corrected breakdown voltage using the group CIGRE 33 with different condition of g, $\%U_{50}/U_{50_0}$ represents the % error between the standard breakdown voltage compare with actual breakdown voltage, A, B, C represents the corrected breakdown voltage using method A, B C respectively in method section, %A, B, C represents the error between standard atmospheric condition breakdown voltage and actual atmospheric condition breakdown voltage in %. Comparison and results of the above methods are shown in figures 4.1 to 4.20 in results sections.

A 20 mm diameter rod with half sphere tip was used for the gap distance of 600 mm. For 1 m discharge path 10 mm hemispherical tip was used [1].

Table 3.4: DC test Rod-plane

H	U_{50}	**IEC**	**%IEC**	U_{50}/U_{50_0}	$\%U_{50}/U_{50_0}$	**A**	**%A**	**B**	**%B**	**C**	**%C**
0.71	475.89	563.96	-2.71	563.28	-0.18	488.18	-13.29	559.15	-0.21	-	-
1.47	468.09	546.89	-5.71	564.48	0.04	481.28	-14.51	534.25	-4.65	-	-
2.16	509.30	586.43	1.11	564.28	0	526.21	-6.53	573.32	2.32	-	-
2.98	514.06	520.60	0.45	564.28	0.07	530.18	-5.83	566.15	1.01	-	-
4.97	527.14	576.04	-0.68	564.28	0.18	537.03	-4.61	554.71	-1	-	-
6.80	544.17	576.01	-0.69	565.29	0.18	545.74	-3.06	553.44	-1.23	-	-
9.30	564.01	580	Ref.	564.28	Ref.	563.02	Ref.	560.32	Ref.	-	-

For a DC tests 320/60 mm toroid was used for gap distance of 0.5 m, 0.75 m and 1 m. Toroid 320/60 where the 320 toroid diameter and 60 mm tube diameter.

Table 3.5: DC test Toroid 320/60-plane gap distance 0.5 meter

H	U_{50}	**IEC**	**%IEC**	U_{50}/U_{50_0}	$\%U_{50}/U_{50_0}$	**A**	**%A**	**B**	**%B**	**C**	**%C**
0.37	272	316.76	10.90	284.70	0	289.21	3.17	294.71	3.17	280.04	0.01
0.98	274	316.93	10.95	284.70	0	292.18	3.55	295.82	3.55	280.07	0.02
1.99	275	315.36	10.40	284.70	0	293.34	3.33	295.82	3.33	280.04	0.01
2.97	277	314.14	9.97	284.70	0	294.35	3.46	295.62	3.48	289.04	3.23
5.84	278	305.01	6.78	284.70	0	288.44	2.13	291.77	2.13	283.29	1.18
10.69	280	285.65	Ref.	284.70	Ref.	284.50	Ref.	285.67	Ref.	280	0

Table 3.6: DC test Toroid 320/60-plane gap distance 0.75 meter

H	U_{50}	**IEC**	**%IEC**	U_{50}/U_{50_0}	$\%U_{50}/U_{50_0}$	**A**	**%A**	**B**	**%B**	**C**	**%C**
0.51	311	381.43	9.26	322.68	-5.90	318.48	-7.15	318.88	-7.22	319.55	-6.29
1.17	309	372.85	6.80	321.31	-6.30	316.65	-7.69	316.26	-7.99	315.39	-7.51
1.93	308	362.97	3.98	320.62	-6.50	315.57	-8	314.68	-8.45	313.63	-8.03
2.72	311	359.95	3.11	322.68	-5.90	318.45	-7.15	317.38	-7.66	325.43	-4.57
4.69	318	353.69	1.32	327.46	-4.50	323.95	-5.56	323.54	-5.87	329.28	-3.44
10.18	341	349.10	Ref.	342.93	Ref.	343.72	Ref.	343.72	Ref.	332.13	-2.60

Table 3.7: DC test Toroid 320/60-plane gap distance 1 meter

H	U_{50}	**IEC**	**%IEC**	U_{50}/U_{50_0}	$\%U_{50}/U_{50_0}$	**A**	**%A**	**B**	**%B**	**C**	**%C**
0.49	432	528.01	7.02	479.11	-2.59	448.86	-8.76	454.95	-7.68	444	-8.83
1.19	426	512.70	3.91	477.65	-2.89	442.91	-9.97	446.50	9.39	434.75	-10.73
2.05	425	502.16	1.78	477.40	-2.94	441.70	-10.22	443.66	-9.97	432.83	-11.12
3.07	431	498.24	0.98	478.87	2.64	447.10	-9.12	448.53	-8.98	449.48	-7.70
5.43	447	493.33	-0.01	482.71	-1.86	458.35	6.83	461.79	-6.29	457.51	-6.06
10.92	487	493.40	Ref.	491.85	Ref.	492	Ref.	492.78	Ref.	458.39	-5.87

Table 3.8: DC test Toroid 320/60-plane gap distance 1 meter 2

H	U_{50}	**IEC**	**%IEC**	U_{50}/U_{50_0}	$\%U_{50}/U_{50_0}$	**A**	**%A**	**B**	**%B**	**C**	**%C**
0.37	460	553.90	15.65	474.03	-1.47	473.41	-1.77	480.90	-0.09	473.28	-1.71
1.02	499	594.81	24.19	485.74	0.97	520.29	7.95	526.80	9.45	509.91	5.90
2.03	452	528.05	10.25	474.17	-1.44	467.87	-2.92	470.21	-2.31	459.91	-4.48
2.97	452.3	519.28	8.42	474.79	-1.31	467.72	2.95	469.33	-2.49	471.95	-1.98
4.87	484.2	536.80	12.08	483.54	0.54	497.73	3.27	501.18	4.13	498.30	3.49
11.37	482	478.95	Ref.	481.09	Ref.	481.95	Ref.	481.31	Ref.	449.12	-6.72

For a DC tests 600/100 mm toroid was used for gap distance of 0.75 m and 1 m. Toroid 600/100 where the 600 toroid diameter and 100 mm tube diameter.

Table 3.9: DC test Toroid 600/100-plane gap distance 0.75 meter

H	U_{50}	**IEC**	**%IEC**	U_{50}/U_{50_0}	$\%U_{50}/U_{50_0}$	**A**	**%A**	**B**	**%B**	**C**	**%C**
1.23	421	480.05	14.56	419.01	1.02	441.36	6.30	421.62	2.25	416.82	1.17
2.93	426	477.89	14.05	421.35	1.58	445.69	7.34	424.93	3.05	422.34	2.51
4.67	416	462.05	10.27	416.67	0.46	429.54	3.45	415.31	0.72	412.99	0.24
10.67	412	419.03	Ref.	414.78	Ref.	415.20	Ref.	412.34	Ref.	410.97	-0.25

Table 3.10: DC test Toroid 600/100-plane gap distance 1 meter

H	U_{50}	**IEC**	**%IEC**	U_{50}/U_{50_0}	$\%U_{50}/U_{50_0}$	**A**	**%A**	**B**	**%B**	**C**	**%C**
0.63	522.50	611.40	15.64	519.54	-0.26	541.33	4.30	510.15	-0.70	517.07	-1.34
1	520.50	608.63	15.12	520.11	0.24	540.91	4.52	509.13	-0.90	515.24	-1.69
3.46	530.20	597.96	13.10	521.88	0.98	549.15	6.11	519.56	1.13	525.87	0.34
4.97	526.20	574.56	8.68	519.44	1.02	535.65	3.50	514.44	1.14	522.52	-0.30
7.21	526.10	553.15	4.63	519.74	0.17	525.88	1.61	515.37	0.37	523.35	-0.32
9.80	524.10	528.69	Ref.	518.86	Ref.	517.51	Ref.	513.74	Ref.	522.42	-0.32

Table 3.11: DC test Sphere 250-plane gap distance 0.5 meter

H	U_{50}	**IEC**	**%IEC**	U_{50}/U_{50_0}	$\%U_{50}/U_{50_0}$	**A**	**%A**	**B**	**%B**	**C**	**%C**
0.43	360	378.04	13.13	352.14	4.98	375.09	13.64	360	9.86	386.25	18.48
2.89	363	382.58	14.49	354.16	5.58	378.33	14.62	363	10.77	390.33	19.74
6.08	329	351.36	5.15	336.35	0.27	335.40	1.61	329	0.40	343.33	5.32
11.06	326	334.16	Ref.	335.45	Ref.	330.06	Ref.	327	Ref.	326.27	0.08

For a DC tests 250 mm diameter sphere was used for gap distance of 0.5 m, 0.75 m and 1 m.

Table 3.12: DC test Sphere 250-plane gap distance 0.75 meter

H	U_{50}	**IEC**	**%IEC**	U_{50}/U_{50_0}	$\%U_{50}/U_{50_0}$	**A**	**%A**	**B**	**%B**	**C**	**%C**
0.66	385	463.13	16.59	391.73	-0.40	404.32	2.02	385	-1.40	413.16	6.49
1.04	388	463.47	16.67	393.32	0	408.28	3.28	388	-0.63	416.51	7.35
2.13	390	459.93	15.78	394.38	0.27	410.55	3.86	390	0.12	419.07	8.01
2.97	391	456.29	14.87	394.91	0.40	410.56	3.86	391	0.14	420.47	8.37
7.09	388	422.43	6.34	393.32	0	396.82	0.386	388	-0.63	401.50	3.48
11.04	388	397.23	Ref.	393.32	Ref.	395.29	Ref.	390.47	Ref.	388.38	0.10

Table 3.13: DC test Sphere 250-plane gap distance 1 meter

H	U_{50}	**IEC**	**%IEC**	U_{50}/U_{50_0}	$\%U_{50}/U_{50_0}$	**A**	**%A**	**B**	**%B**	**C**	**%C**
0.41	448.2	540.44	12.30	470.41	-2.22	461.48	-4.08	448.20	0.50	480.87	0.14
1.95	445	518.80	7.08	469.36	-2.44	458.90	-4.61	445	-0.22	478.09	-0.44
2.66	448	516.77	7.38	471.89	-1.92	462.94	-3.77	448	0.45	481.63	0.30
5.47	456.6	498.54	3.60	474.01	-1.47	464.59	-3.43	456.60	2.38	478.96	-0.26
10.98	480.19	481.24	Ref.	481.10	Ref.	481.12	Ref.	446	Ref.	480.91	0.15

Table 3.14: DC test Sphere 250-plane gap distance 1 meter 2

H	U_{50}	**IEC**	**%IEC**	U_{50}/U_{50_0}	$\%U_{50}/U_{50_0}$	**A**	**%A**	**B**	**%B**	**C**	**%C**
0.66	410	501.14	15.30	425.20	-1.85	425.49	-1.75	410	2.52	439.98	2.56
0.98	408	492.91	13.40	424.35	-2.05	423.59	-2.19	408	2.02	437.96	2.09
2.11	410	480.15	10.47	425.20	-1.85	425.87	-1.66	410	2.52	440.55	2.69
3.07	413	472.87	8.79	426.49	-1.55	428.06	-1.16	413	3.27	442.04	3.04
5.53	419	456.57	5.04	429.02	-0.97	428.89	-0.97	418	4.77	439.28	2.40
10.74	429	434.66	Ref.	433.22	Ref.	433.09	Ref.	400	Ref.	430.54	0.36

3.2.8 Switching Impulse Test

For a distance of 600 mm, a 20 mm diameter rod with a half spherical tip was used. A 10 mm hemispherical tip rod was used for the 1 and 2 m gap distances.

Table 3.15: Switching impulse Rod-plane gap 0.5 meter

H	U_{50}	**IEC**	**%IEC**	U_{50}/U_{50_0}	$\%U_{50}/U_{50_0}$	**A**	**%A**
1.05	279	321.18	-0.04	283.57	-13.05	303.12	-8.69
7.58	294	313.23	-2.51	284.04	-12.90	312.38	-5.90
10.5	274	321.31	Ref.	326.12	Ref.	332	Ref.

Table 3.16: Switching impulse test Rod-plane gap 1 meter

H	U_{50}	**IEC**	**%IEC**	U_{50}/U_{50_0}	$\%U_{50}/U_{50_0}$	**A**	**%A**
0.46	436	489.72	7.58	450.54	-1.54	453.11	-2.34
2.08	460.9	514.56	13.04	461.54	0.86	483.06	4.11
6.53	440	463.36	1.79	454.06	-0.77	454.48	-2.04
11.72	454	455.21	Ref.	457.60	Ref.	464	Ref.

Table 3.17: Switching impulse test Rod-plane gap 2 meter

H	U_{50}	**IEC**	**%IEC**	U_{50}/U_{50_0}	$\%U_{50}/U_{50_0}$	**A**	**%A**
0.45	722	779.93	2.59	739.26	-2.52	740.77	-3.32
1.79	733.59	790.06	3.92	748.88	-1.25	755.21	-1.43
6.09	739.70	767.24	0.92	750.41	-1.05	755.48	-1.40
10.66	754.40	760.28	Ref.	758.38	Ref.	766.24	Ref.

A 150 mm diameter sphere with a gap spacing of 600mm was used for switching impulse voltage experiments.

Table 3.18: Switching impulse test Sphere 150-plane gap 0.6 meter

H	U_{50}	**IEC**	**%IEC**	U_{50}/U_{50_0}	$\%U_{50}/U_{50_0}$	**A**	**%A**
1	266.20	310.34	-0.03	303.40	0.07	292.36	-6.24
8	288.20	310.43	Ref.	303.18	Ref.	311.84	Ref.

Three toroid dimensions were tested for switching impulse voltage experiments. Toroids with dimensions of 350 mm outer diameter and 100 mm tube diameter (350/100), and 425 mm outer diameter and 75 mm tube diameter (425/75) were used at gap distances of 600 mm. For lengths of 1 and 2 m, the toroid parameters were 600 mm outer diameter and 100 mm tube diameter (600/100).

Table 3.19: Switching impulse test Toroid 350-plane gap 0.6 meter

H	U_{50}	**IEC**	**%IEC**	U_{50}/U_{50_0}	$\%U_{50}/U_{50_0}$	**A**	**%A**
0.85	354	409	10.44	367.68	1.73	377.95	3.58
6.40	351	383.80	3.63	360.10	-0.37	364.35	-0.14
11.10	354	370.34	Ref.	361.10	Ref.	364.88	Ref.

Table 3.20: Switching impulse test Toroid 425-plane gap 0.6 meter

H	U_{50}	**IEC**	**%IEC**	U_{50}/U_{50_0}	$\%U_{50}/U_{50_0}$	**A**	**%A**
0.8	339	377.07	8.76	332.80	-2.32	347.35	1.13
4	335	367.24	5.90	331.54	-2.69	342.92	-0.15
11	337	346.70	Ref.	340.70	Ref.	343.45	Ref.

Table 3.21: Switching impulse test Toroid 600-plane gap 1 meter

H	U_{50}	**IEC**	**%IEC**	U_{50}/U_{50_0}	$\%U_{50}/U_{50_0}$	**A**	**%A**
0.39	485.17	551.58	5.05	512.77	-1	513.17	-3.24
0.94	490.86	554.98	5.69	513.91	-0.78	519.60	-2.02
2.04	492.42	549.88	4.72	514.12	-0.74	519.96	-1.96
3.05	498.83	552.41	5.20	516.43	-0.29	527.79	-0.48
5.29	501.21	541.75	3.17	516.85	-0.21	527.59	-0.52
9.69	508.75	525.08	Ref.	517.96	Ref.	530.36	Ref.

Table 3.22: Switching impulse test Toroid 600-plane gap 2 meter

H	U_{50}	**IEC**	**%IEC**	U_{50}/U_{50_0}	$\%U_{50}/U_{50_0}$	**A**	**%A**
0.38	756.10	822.55	5.18	736.13	-5.26	777.05	-1.17
0.83	746.30	806.38	3.11	728.27	-6.27	765.87	-2.59
2.04	741.10	796.27	1.81	729.37	-6.13	762.31	-3.04
3.08	746.50	796.88	1.89	752.63	-3.14	768.03	-2.31
5.26	758.70	797.45	1.97	746.82	-3.89	779.53	-0.85
10.12	769.70	782.08	Ref.	777.01	Ref.	786.27	Ref.

4

Results

Figures. 4.2 to 4.20 represents the result of the DC and Impulse test methods. There are four methods for DC and two methods for impulse shown in figure along with IEC 60060 correction method.The different colour letters in the figures show the % error when compared the corrected breakdown voltage to the breakdown voltage under standard atmospheric conditions. Figures. represents the U_{50} and $U_{50_{corrected}}$ as a function of absolute humidity h to relative air density δ.

4.1 DC Results

Different fit functions apply to the geometry and this thesis attempt to get an appropriate equation for calculation of humidity correction parameter (k). Throughout the thesis, it was observed that there is no similar fit function that is applicable to one or more geometry. The fit function used for the 320 mm diameter toroid with the plane does not match the fit function used for the 600 mm diameter toroid with the plane. As a result, an individual approach for individual geometry has been devised, it is mentioned in the methods section. The final fit function and their corresponding equation coefficients are represented in Table 4.1. The coefficients a, b, c, and d were calculated using the MATLAB fit function with proper input data and output.

Here, table 4.1 represents the final equation for each geometry as well as different humidity conditions. The absolute humidity condition is divided into two parts. The absolute humidity $< 3\ g/m^3$ consider as lower humidity condition and $> 3\ g/m^3$ consider as higher humidity condition. The best fitting for rod-pane and toroid 320-plane are polynomial of 2^{nd} order. Whereas the best fitting for the toroid 600-plane and sphere 250-plane is exponential of 1^{st} order. Table 4.1 it type represents the best fit function, Eq.'s to calculate k parameters shows the equation to estimate the value of k as per geometry condition and absolute humidity condition, coefficient represents the sample equation of the fit type.

Table 4.1: DC equations as per the geometry and humidity condition

MATLAB Fit function				
Geometry	**Humidity**	**Fit type**	**Eq.'s to calculate k parameter**	**Coefficient**
Rod-plane	-	Poly2	$1 + 0.018 * (h/\delta)$-0,00022$(h/\delta)^2$	c+bh+a$(h\delta)^2$
Toroid320-plane	>3	Poly2	$0.96 + 0.018 * h - 0.0048 * h^2$	c+bh+ah^2
Toroid320-plane	<3	Poly2	$0.001 * h^2 + 0.0008 * h + 0.95$	c+bh+ah^2
Toroid600-plane	-	Expo1	$1.011 * (e^{-0.000785*h})$	a*e^{bh}
Sphere-plane 250	<3	Expo1	$0.93 * (e^{-0.0009*h})$	a*e^{bh}
Sphere-plane 250	>3	Expo1	$0.91 * (e^{0.0084*h})$	a*e^{bh}

4.1.1 Rod-Plane

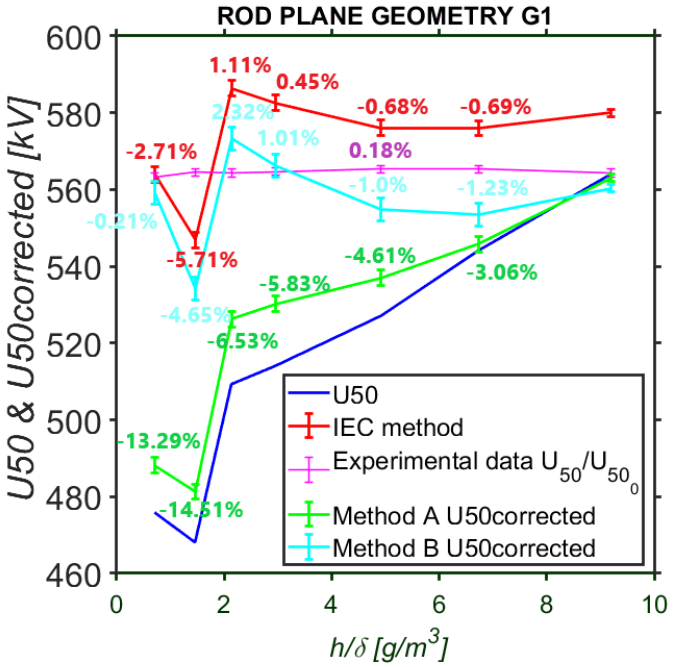

Figure 4.1: Rod-plane gap distance 1 m

For rod-plane geometry it is observe that the current IEC method is more accurate.

4.1.2 Toroid 320-Plane

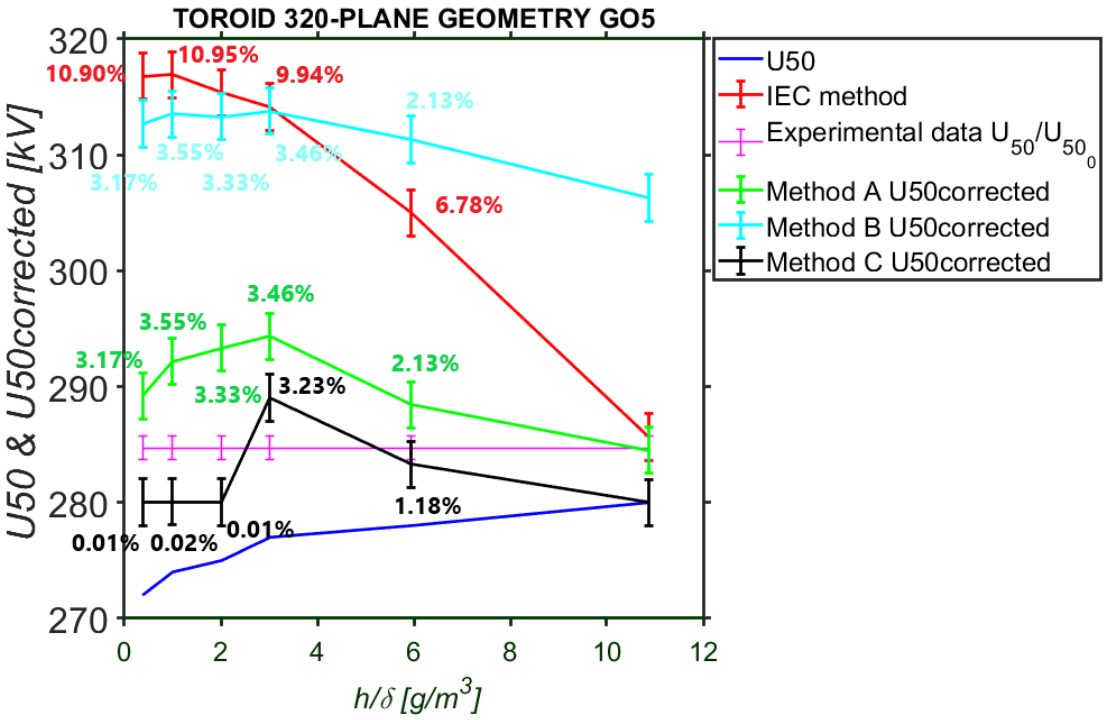

Figure 4.2: Toroid 320-plane gap distance 0.5 m

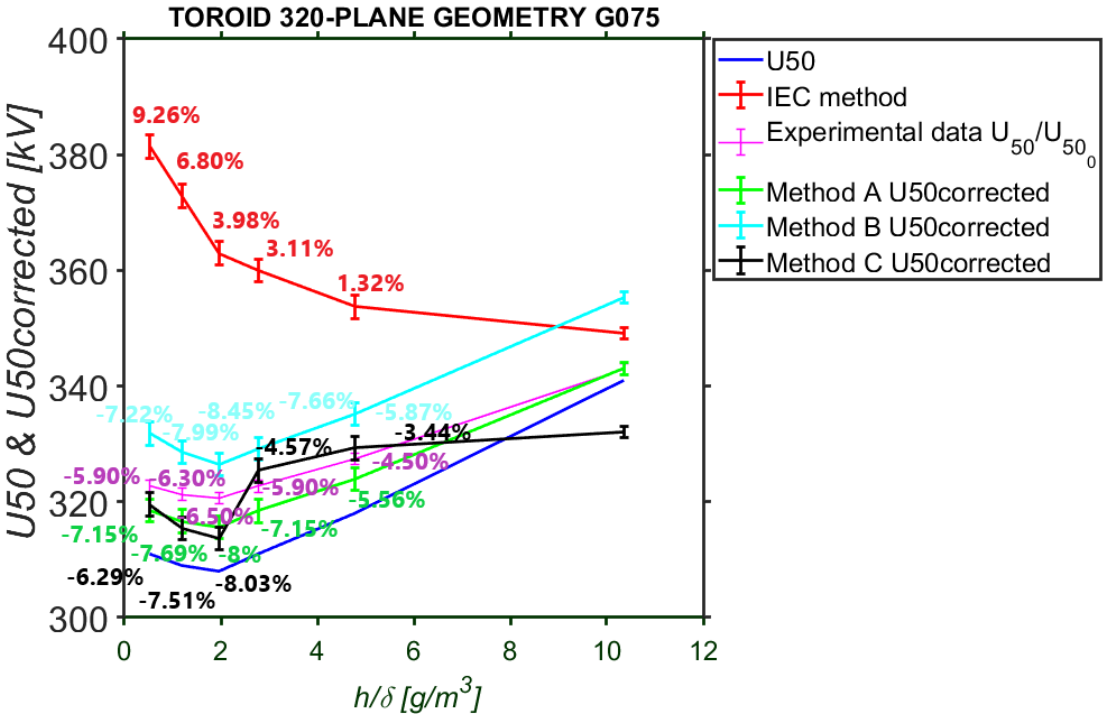

Figure 4.3: Toroid 320-plane gap distance 0.75 m

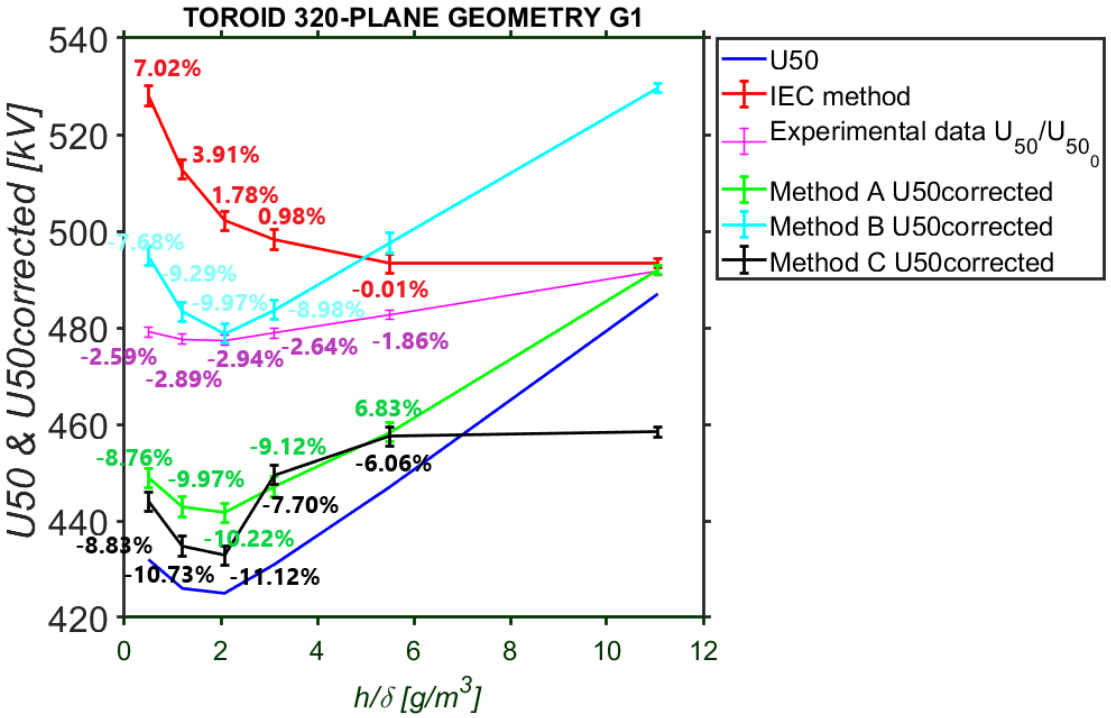

Figure 4.4: Toroid 320-plane gap distance 1 m

For toroid 320-plane geometry it is observed that for the discharge path of 0.5 m method C is more accurate but for the discharge path of 0.75 m and 1m, none of the above methods are accurate. From figure 4.2 to 4.4 it is observed that the experimental value of breakdown voltage has a larger variation compared with the standard atmospheric condition and it has a small variation in the discharge path of 0.5 m It could be because when the gap is small the field becomes more uniform and the formation of streamer required less energy for breakdown. Whereas for the long gap distance the formation from steamer to avalanche will take more time [**?**]. But when the electric field becomes more uniform the corrected breakdown voltage has a larger variation at lower humidity conditions. As a result the more breakdown could happen at low absolute humidity. The breakdown mainly affected by the absolute humidity [1] [2].

4.1.3 Toroid 600-Plane

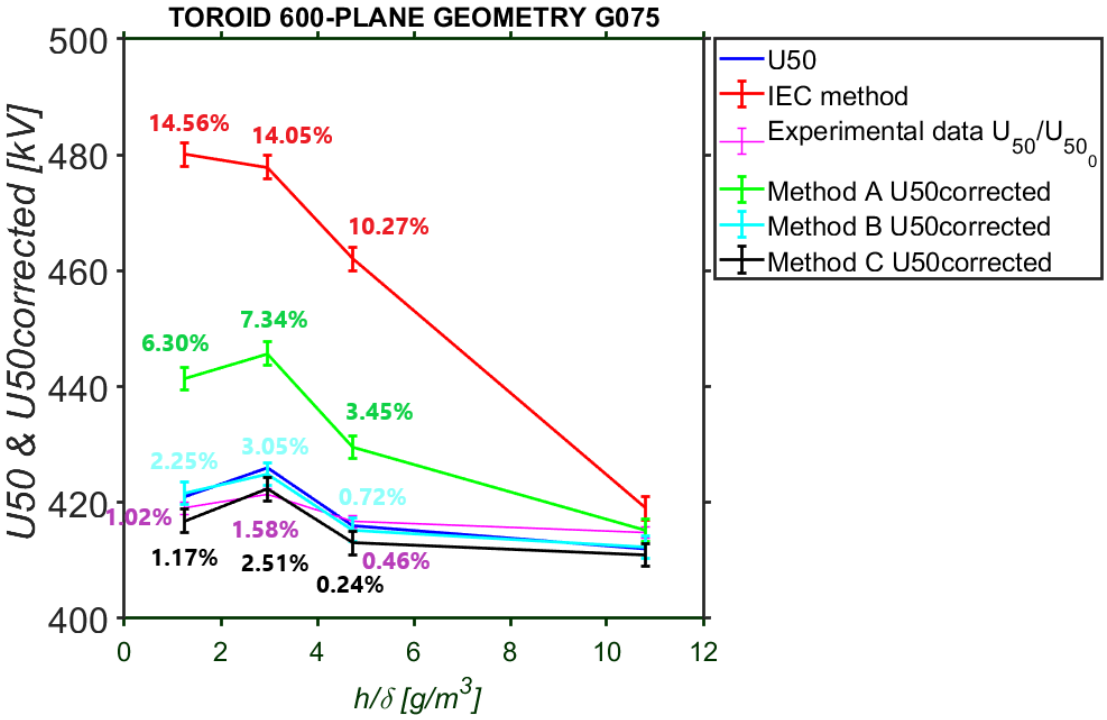

Figure 4.5: Toroid 600-plane gap distance 0.75 m

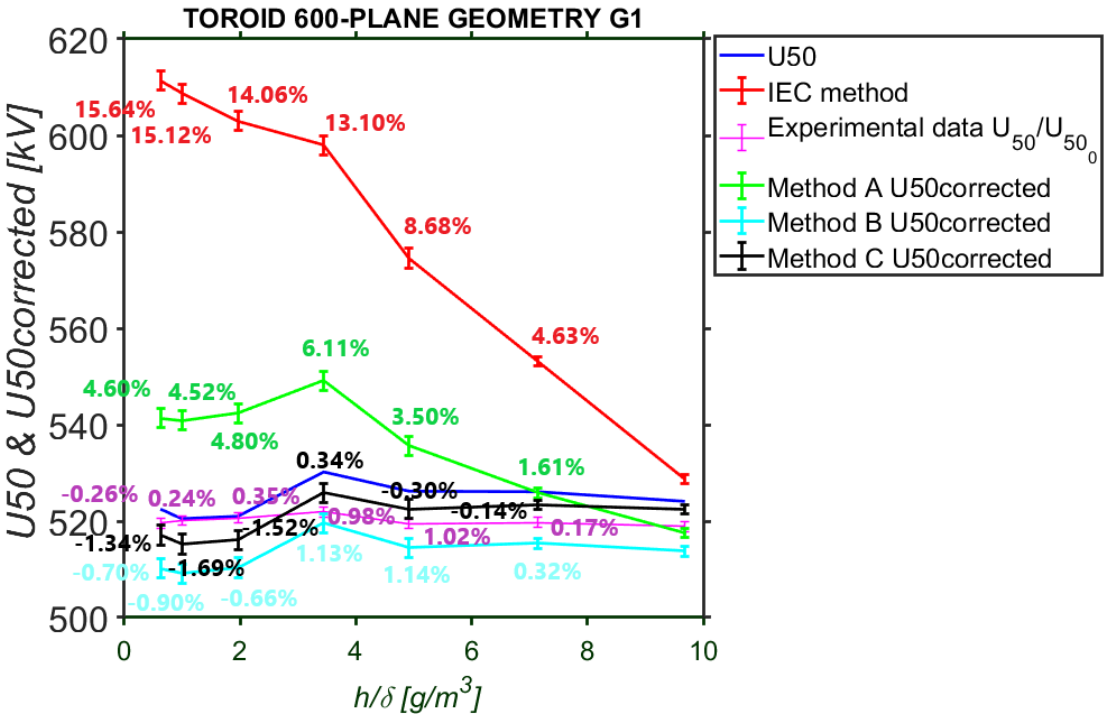

Figure 4.6: Toroid 600-plane gap distance 1 m

Figure 4.5 and 4.6 represents the results of different method used in method section. It is observed that for geometry toroid 600-plane Method C has maximum 1.69% error in $U_{50_{Corrected}}$. The small negative variation in voltage level is due to unavailability of the standard atmospheric condition.

4.1.4 Sphere 250-Plane

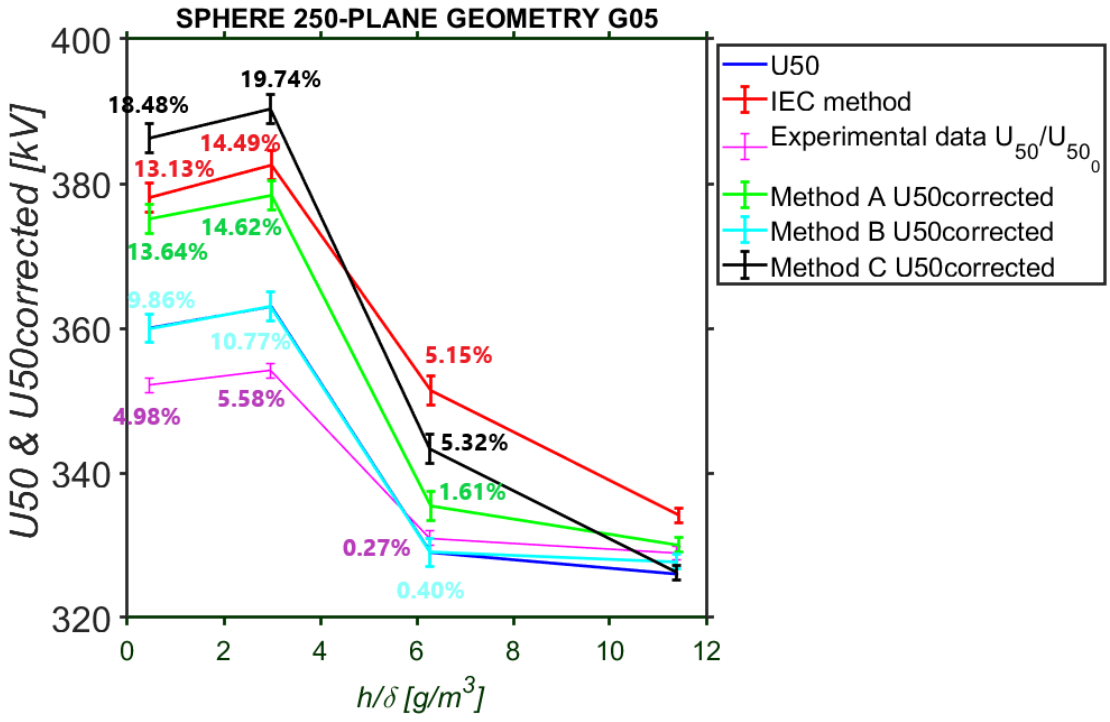

Figure 4.7: Sphere 250-plane gap distance 0.5 m

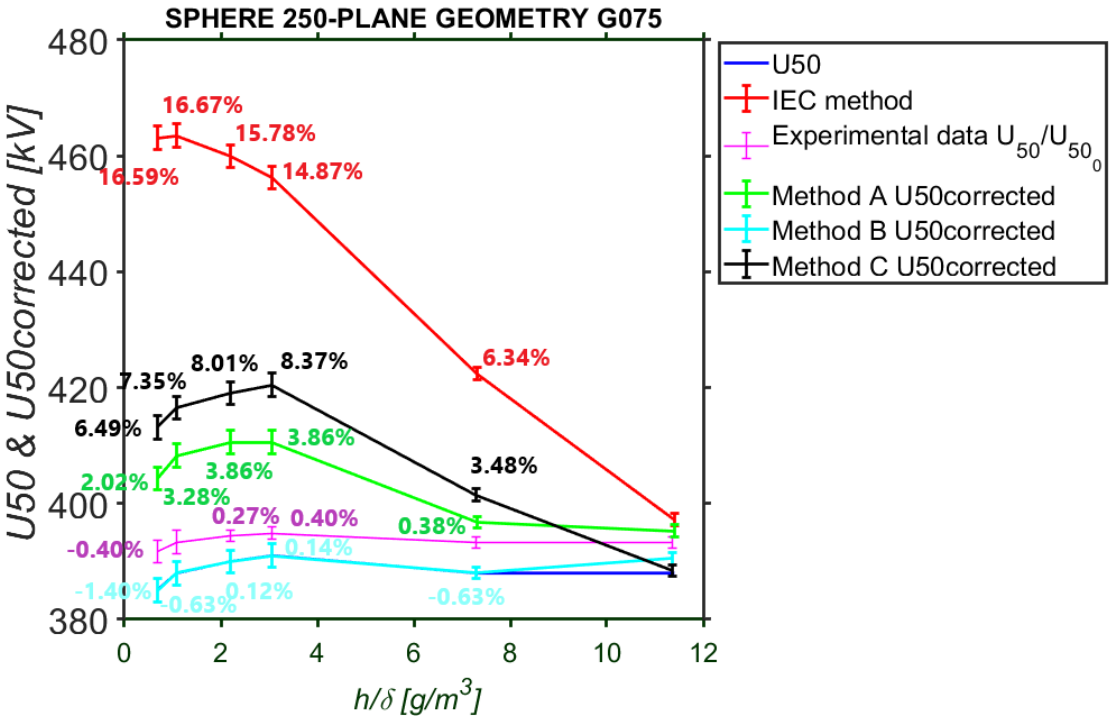

Figure 4.8: Sphere 250-plane gap distance 0.75 m

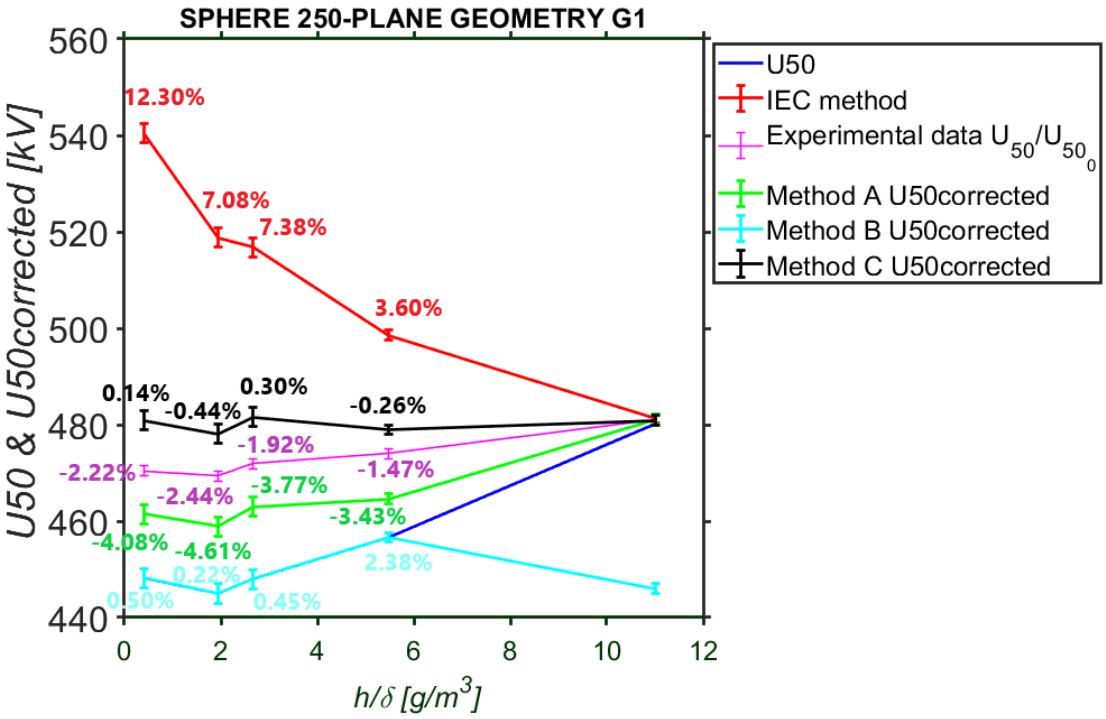

Figure 4.9: Sphere 250-plane gap distance 1 m

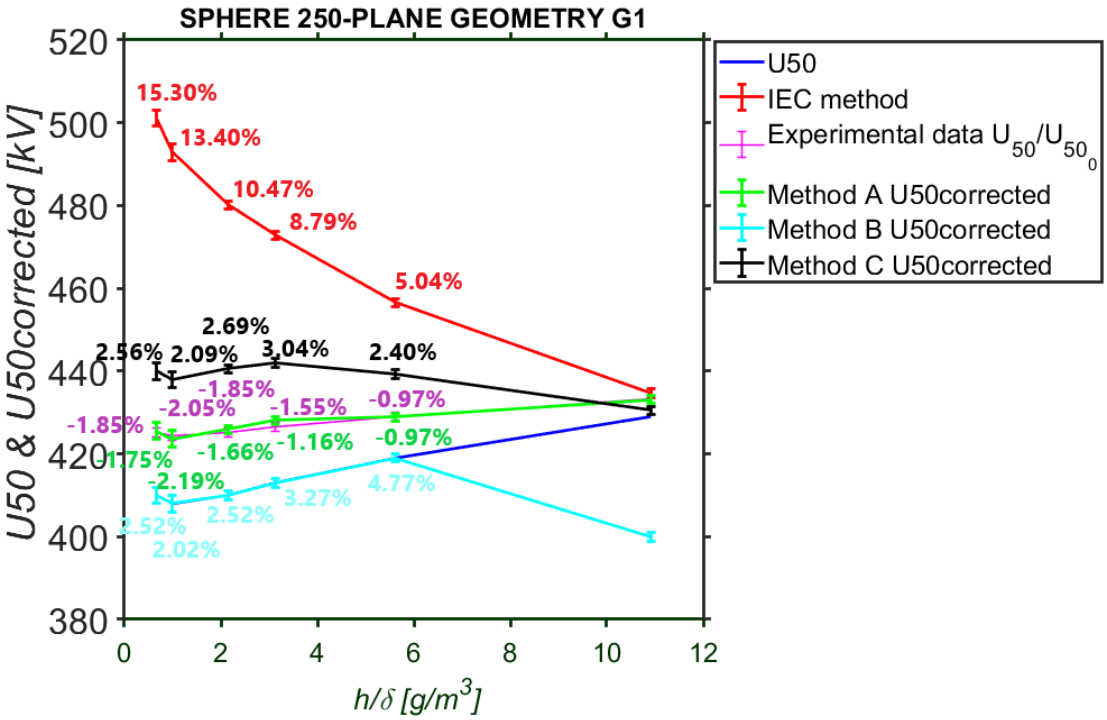

Figure 4.10: Sphere 250-plane gap distance 1 m 2

From figure 4.8 and 4.10 represents the sphere 250-plane with different discharge path. It is observed that method D is more accurate for sphere 250-plane geometry. Sphere 250-plane has maximum -4.61% error with method B and maximum 8% error with method C. In contrast, the IEC correction approach has a maximum error of 16.67% percent for the sphere 250-plane, which is greater than the errors for methods B and C.

Also, it is observed that the IEC method has over-correction during the extremely low humidity condition i.e. $h/\delta < 2\ g/m^3$ the corrected breakdown voltage $U_{50_{Corrected}}$ at actual atmospheric condition is increasing with a reference of standard humidity condition during low humidity. This behavior is noticeable in non-uniform arrangements such as rod-plane gap, sphere-plane, and toroid-plane (320/60). For quasi-uniform arrangements like toroid-plane (600/100), the changes in the slope are significant, and an almost constant linear behavior has observed. Overall for all the available geometry data methods, C is more accurate compared with other IEC methods. There are 3% to 4% variations in voltage difference due to the unavailability of the standard atmospheric breakdown voltage.

4.2 Impulse test

This section represents the Impulse test where the regression analysis applies to one or more geometries as well. The data available for the switching is positive switching impulse data. Whereas it has only two methods experimental data U_{50}/U_{50_0} and A. Experimental data U_{50}/U_{50_0} has been developed by the CIGRE 33 group [40]. Method A has been developed using the machine learning tool. Eq. 3.15 represents the equation for method A. Table 4.2 represents the final equations for the different geometries. It is also observed that the method developed by the CIGRE 33 group was also the best fitting for all the geometry with varied discharge paths.

Table 4.2: SI equations as per the geometry

MATLAB Fit function				
Geometry	**Discharge path (m)**	**Fit type**	**Eq.'s to calculate k parameter**	**Method**
Rod-plane	0.6	Poly2	$1 + 0.010 * (h/\delta)$-0,00022$(\mathrm{h}/\delta)^2$	IEC 60060
Rod-plane	>1	Poly2	0.9786 * EXP $\left(0.002509 * \left(\frac{\mathrm{h}}{\delta} - 11\right)\right)$	Method A
Toroid 350-plane	-	Expo1	0.9786 * EXP $\left(0.002509 * \left(\frac{\mathrm{h}}{\delta} - 11\right)\right)$	Method A
Toroid 425-plane	-	Expo1	0.9786 * EXP $\left(0.002509 * \left(\frac{\mathrm{h}}{\delta} - 11\right)\right)$	Method A
Toroid 600-plane	-	Expo1	0.9786 * EXP $\left(0.002509 * \left(\frac{\mathrm{h}}{\delta} - 11\right)\right)$	Method A
Sphere 150-plane	-	Poly2	$1 + 0.010 * (h/\delta)$-0,00022$(\mathrm{h}/\delta)^2$	IEC 60060
Sphere 500-plane 250	-	Poly2	$1 + 0.010 * (h/\delta)$-0,00022$(\mathrm{h}/\delta)^2$	IEC 60060

4.2.1 Rod-Plane

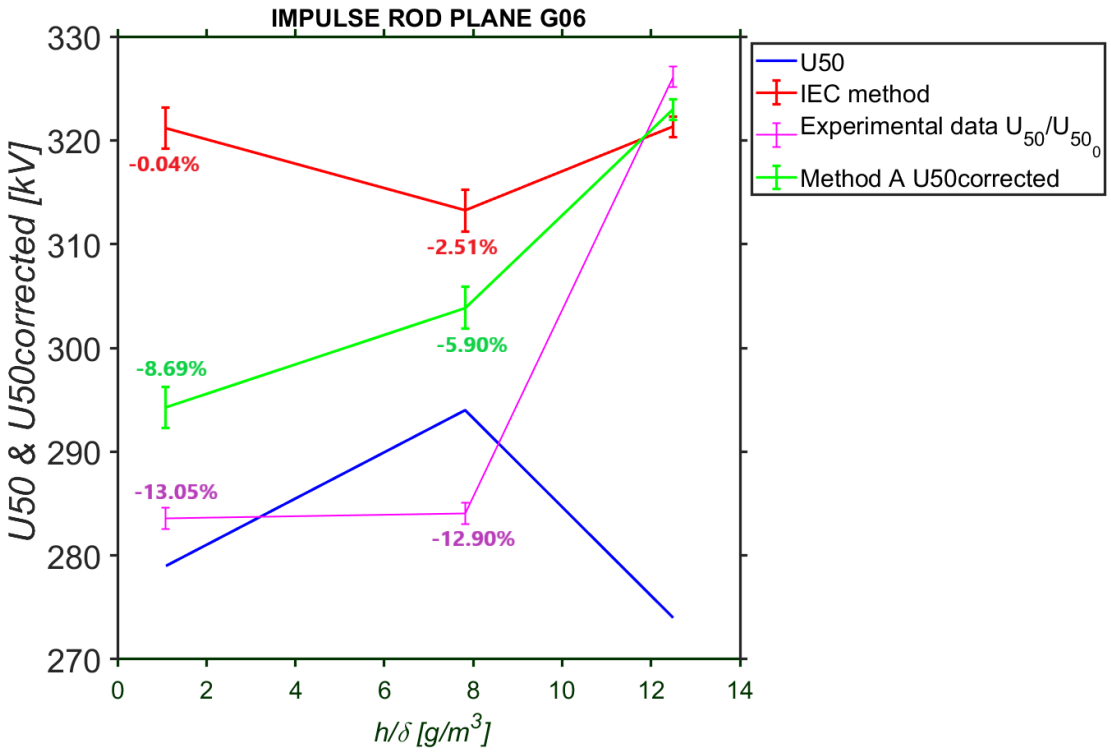

Figure 4.11: Rod-Plane gap distance 0.6 m

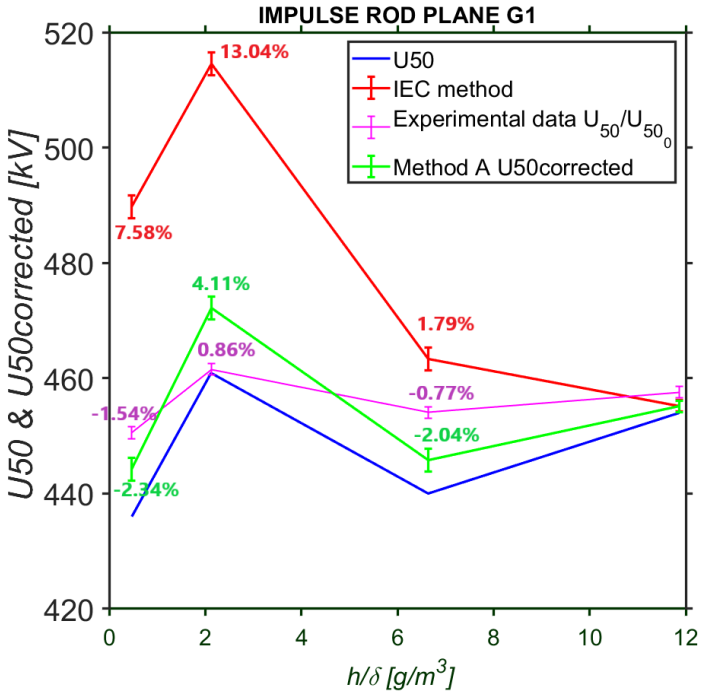

Figure 4.12: Rod-Plane gap distance 1 m

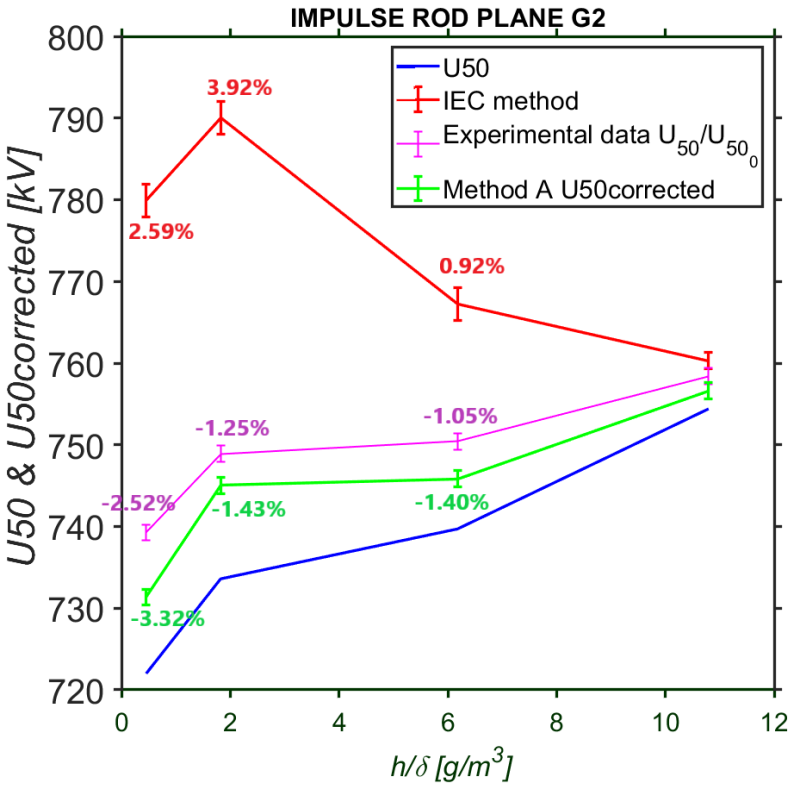

Figure 4.13: Rod-Plane gap distance 2 m

From figure 4.11 to 4.13 represents rod-plane geometry with 0.6, 1, and 2 meter discharge path. For discharge path, 0.6 m IEC method is more accurate and for >= 1 m method A is more accurate. Figure 4.12 indicates that the IEC correction method has an over-correction of 13.04% for gap distance 1 m. It is observed that for the humidity $>2g/m^3$ the corrected breakdown voltage has only a 1.79% error found as compared with the standard atmospheric condition breakdown voltage. The major variation in corrected breakdown voltage $U_{50_{corrected}}$ comes from the absolute humidity $<2g/m^3$.

4.2.2 Toroid-plane

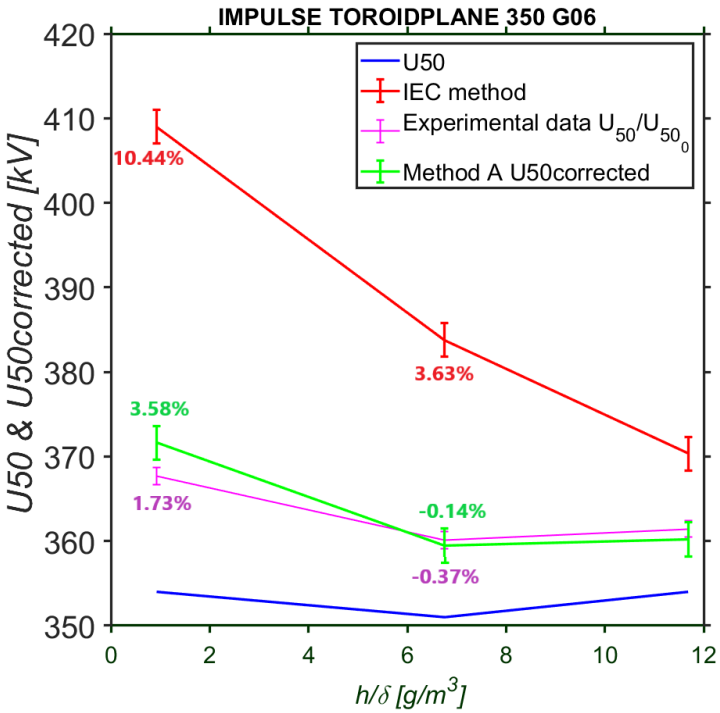

Figure 4.14: Toroid 350-Plane gap distance 0.6 m

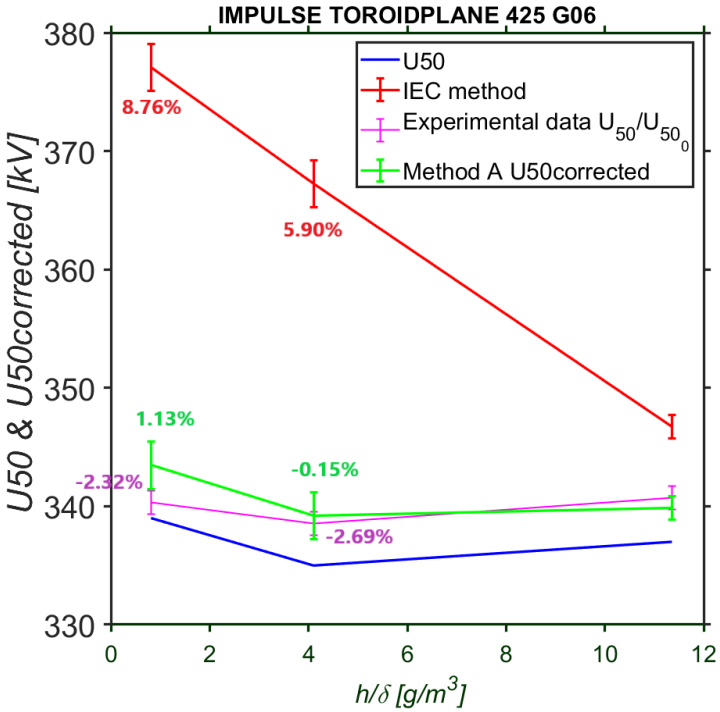

Figure 4.15: Toroid 425-Plane gap distance 0.6 m

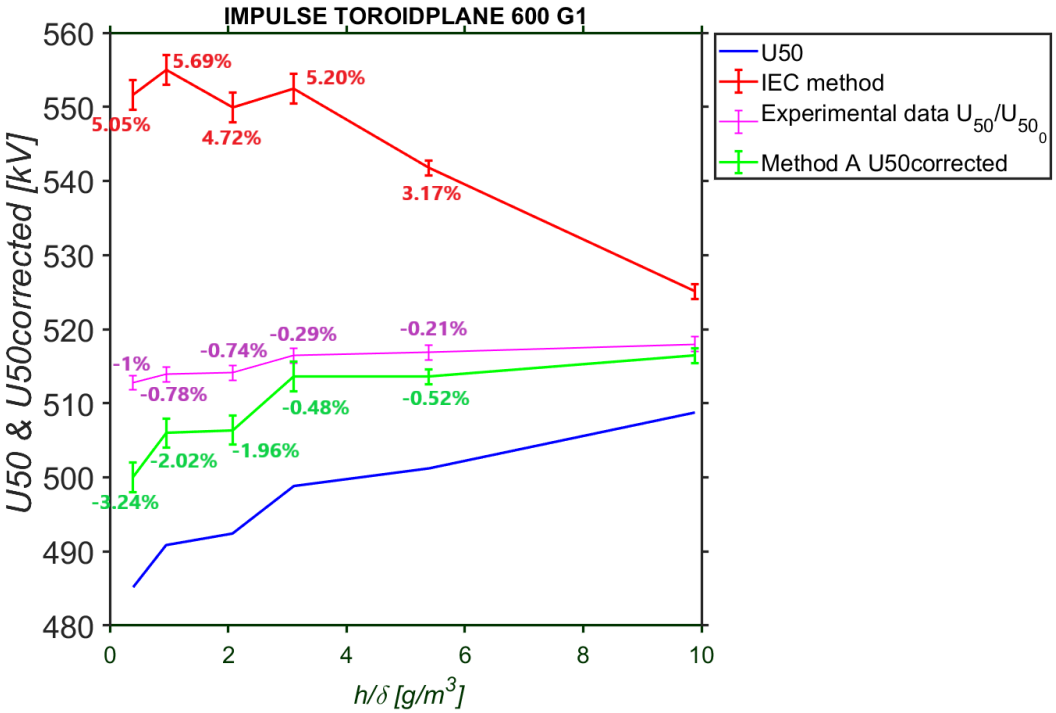

Figure 4.16: Toroid 600-Plane gap distance 1 m

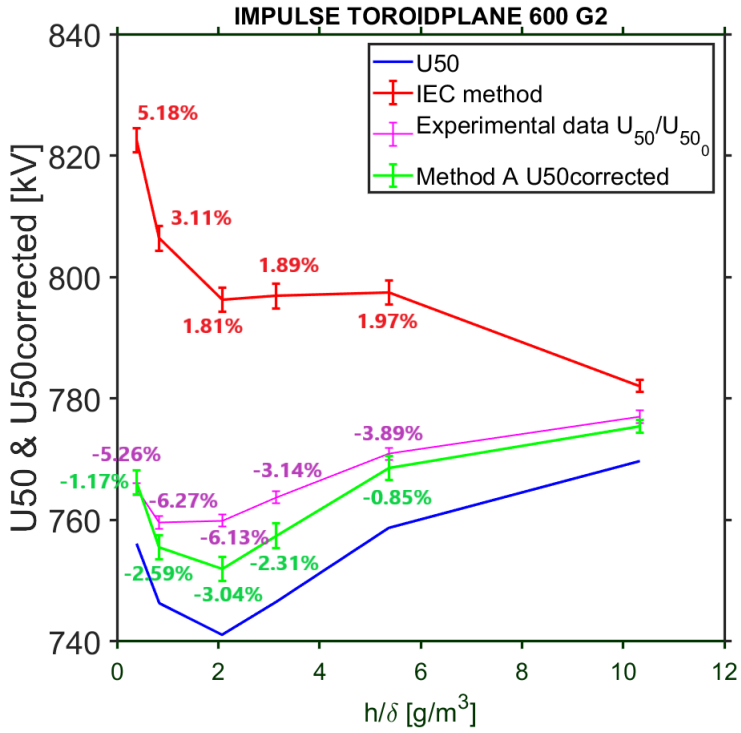

Figure 4.17: Toroid 600-Plane gap distance 2 m

The toroid-plane geometry method A is more accurate for all the different diameters of toroids. The variation in IEC 60060 $U_{50Corrected}$ for toroid 350 plane has over-

correction at lower humidity condition is about 10.44% which is higher than method A. In the low humidity condition method A has only a 3.54% error. This variation is due to the unavailability of the standard atmospheric condition breakdown voltage. A further observation in the toroid-plane geometry is that the corrected breakdown voltage ($U_{50Corrected}$) decreases with increasing toroid diameter and discharge path which is also observed in method A.

4.2.3 Sphere-Plane

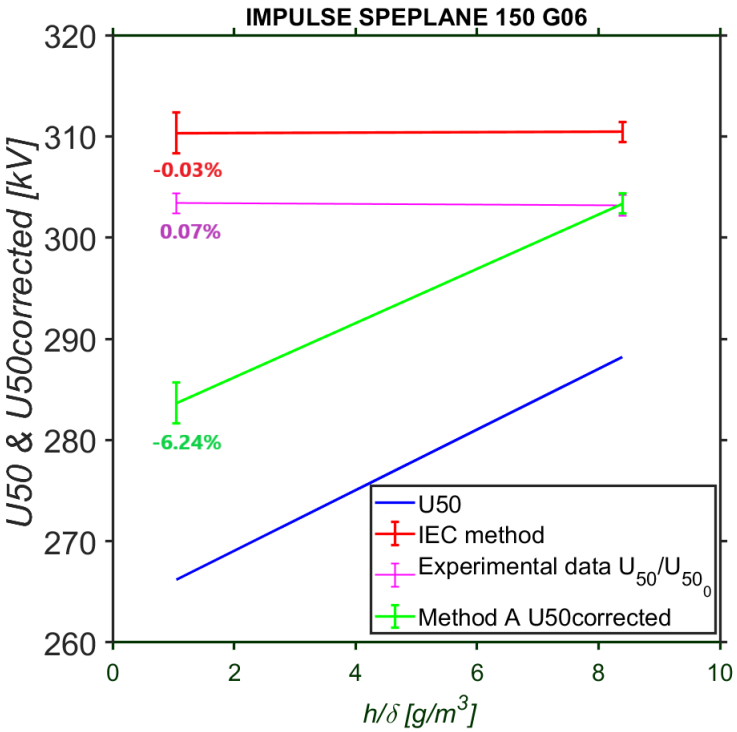

Figure 4.18: Sphere 150-Plane gap distance 0.6 m

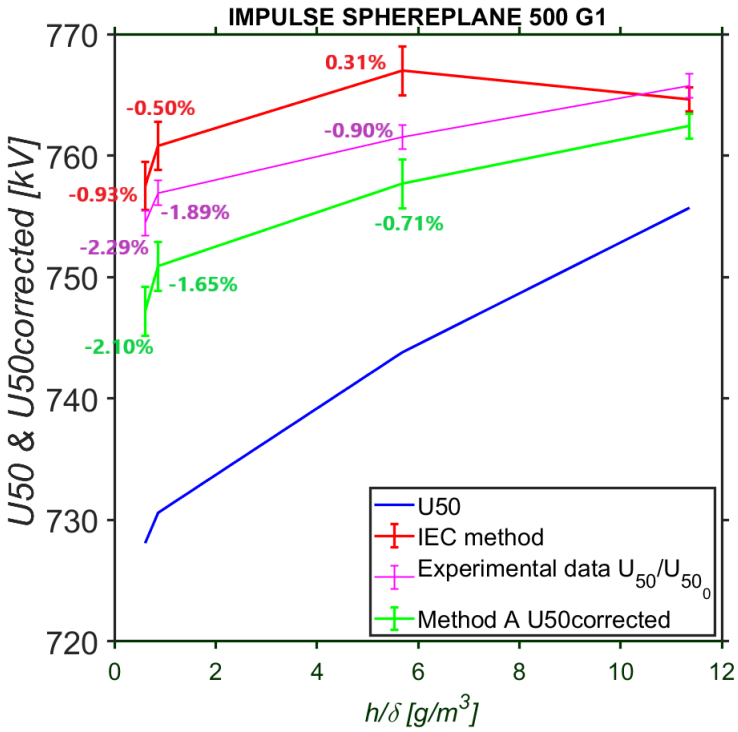

Figure 4.19: Sphere 500-Plane gap distance 1 m

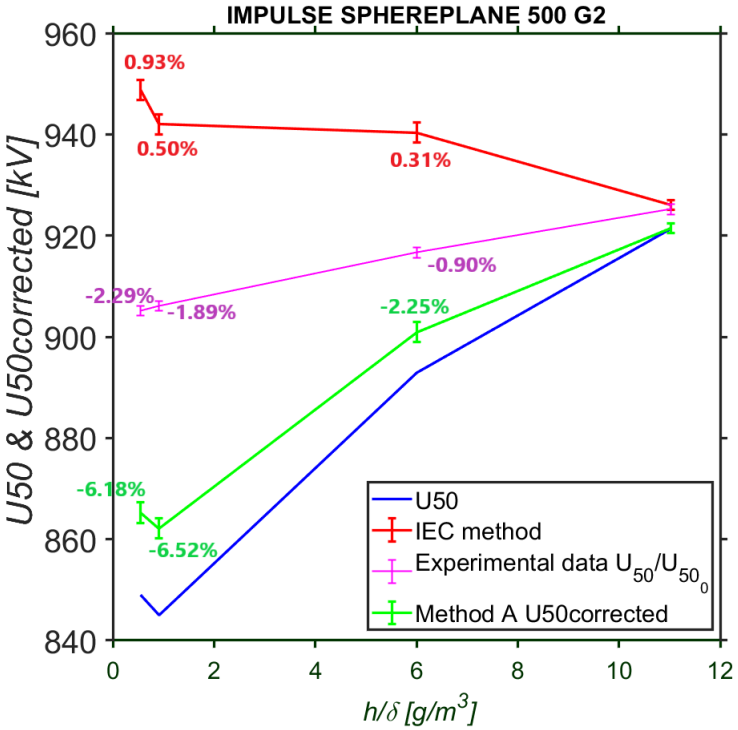

Figure 4.20: Sphere 500-Plane gap distance 2 m

Figure 4.18 to 4.20 shows two different spheres of 150 and 500 mm diameter which were used for the switching impulse test. It is observed that for sphere-plane geometry current IEC method is more accurate. For the sphere-plane geometry IEC correction method has only 0.93% variation in corrected breakdown voltage. Sphere-plane is a non-uniform arrangement in which the experimental breakdown voltage is significantly decreasing with decreasing humidity with respect to air density δ. As compare with previous arrangements where experimental breakdown voltage did not decrease significantly. The corrected breakdown voltage using IEC method has very small over-correction which has been observed with the positive switching impulse voltage.

5

Conclusion

It was observed during the thesis that the IEC 60060 method used the pre-discharge value g to calculate the exponent m and w. In major results the deviation in air density factor which is very small. So, the value of the air density correction factor k_1 will be always closer to 1 which is not major affecting to the correction factor. Where, the humidity correction factor parameter (k) is depends on the geometry, electric field conditions, degree of humidity, temperature, and pressure among others. Therefore a general equation to cover all possible geometries can introduce a larger percentage error on the corrected breakdown voltage. So, to get a less percentage of corrected breakdown voltage it was divided as per the experimental breakdown voltage behaviour. In case of non-uniform the experimental breakdown voltage was increase with at extreme low humidity condition as a result it was divided in two region and applied a machine learning technique. Regression analysis apply to low humidity condition and high humidity condition where it was observed that the general equation is not possible to discover all the geometries in one equation. As a result it was divided into two parts with the humidity level $<3g/m^3$ and $>3g/m^3$ which introduce the small percentage of error on the corrected breakdown voltage. For a DC and Switching impulse the best fit equation was obtain from the regression analysis tool with help of MATLAB machine learning tool. It was also observed that, method proposed by the CIGRE 33 group to calculate the humidity correction parameter (k) has less % error in calculation of corrected breakdown voltage. But the drawback in that method was only to known the standard atmospheric condition breakdown voltage for a particular discharge path and geometry configuration before generalized.

The final equations for DC and Switching impulse test is mentioned in table 4.1 and 4.2 respectively. During the regression analysis it was observed that the major factor affecting to the corrected breakdown voltage was humidity correction. It was also observed that with small no. of data the machine learning tool shows the higher degree of confidence, due to this inaccuracy in equation has been raised. It is rec-

ommended to check this method with large no. of data sets so more test campaign are required to get large no. of data set. Further, study required to understand influence of humidity on air insulation for other discharge paths.

5.0.1 Limitation

There are several limitation during this master thesis which are as follows:

- Data availability is very less to use machine learning technique
- There are no other alternatives in machine learning i.e. Python and R Programming. Which, helps to produce the result with the small data
- A machine learning (Python & R Programming) tool is only applicable to huge data sets and has the limitation of not providing any equations
- In individual geometry, the machine learning tool recommends Gaussian fitting as the best fit, which results in a deviation when the input data changes
- The machine learning tool only provides a predicted value of the model based on the past algorithm's understanding
- There is no data available for the A.C. test correction method, hence this master thesis suggestion is solely applicable to D.C. testing and impulse testing correction methods
- New proposed method is only applicable to configuration shows in this paper, for the other geometry configuration it is better to check available equations or create equations using same technique

Bibliography

[1] L. Arevalo, D. Wu, O. Diaz, M. Larsson, and C. Tornkvist, "Influence of extreme low humidity on the dielectric strength of air insulation under critical design voltages," Ludvika, 2019.

[2] L. Arevalo, D. Wu, and M. Larsson, "DC AIR HUMIDITY CORRECTION FACTOR FOR," pp. 1–6.

[3] D. Wu, G. Asplund, B. Jacobson, M. Li, and F. Sahlen, "Humidity influence on switching-impulse breakdown voltage of air gaps for indoor high-voltage installations," 14Th Int. Symp. High Volt. Eng., pp. 3–6, 2005.

[4] L. Arevalo, D. Wu, and M. Larsson, "Air humidity factor for external insulation under positive switching impulses - Revisited," Lect. Notes Electr. Eng., vol. 599 LNEE, pp. 784–794, 2020,

[5] Mikropoulos, P. N., Stassinopoulos, C. A., Mikropoulos, P. N., Bagavos, C. J. (1992). Positive impulse humidity correction factor for medium rod-plane gaps Soil ionization View project Stochastic (fractal-based) simulation modeling for lightning protection studies View project POSITIVE IMPULSE HUMIDITY CORRECTION FACTOR FOR MEDIUM ROD-PI'ANE GAPS (Vol. 2)

[6] Wu, D., Asplund, G., Jacobson, B., Li, M., Sahlen, F. (n.d.). Humidity influence on switching-impulse breakdown voltage of air gaps for indoor high-voltage installations

[7] https://www.datarobot.com/wiki/fitting/ (fitting function)

[8] Mostajabi, A. H., Samimi, M. H., Arabzadeh, M., Akmal, A. A. S., Mohseni, H. (n.d.). EFFECT OF HUMIDITY ON THE BREAKDOWN VOLTAGE OF INSULATORS AT VARYING HUMIDITY AND TEMPERATURE CONDITIONS

[9] T. Tsuboi, G. Ueta, S. Okabe, Y. Shimizu, T. Ishikura, and E. Hino, "K-factor value and front-time-related characteristics in negative polarity lightning impulse test for UHV-class air insulation," IEEE Trans. Power Deliv., vol. 28, no. 2

[10] Z. Tanasic, M. Schueller, M. Bucher, J. Smajic, L. Zehnder, and T. Werder-, "20th INTERNATIONAL SYMPOSIUM ON HIGH VOLTAGE ENGINEERING,"2017.

[11] D. W. Sun, Y. Zhou, T. Nian, and L. Li, "Research on the Insulation Performance of New Environmentally Friendly Insulation Gas Hexafluoropropylene and Carbon Dioxide Mixed Gas," IOP Conf. Ser. Earth Environ. Sci., vol. 781, no. 5, 2021,

[12] P. Simón, F. Garnacho, S. M. Berlijn, and E. Gockenbach, "Determining the test voltage factor function for the evaluation of lightning impulses with oscillations and/or an overshoot," IEEE Trans. Power Deliv., vol. 21, no. 2, pp. 560–566, 2006,

[13] B. Sékongo et al., "Pre-breakdown and breakdown behavior of synthetic and natural ester liquids under AC stress," Energies, vol. 15, no. 1, pp. 1–10, 2022,

[14] U. Schubert, A. Shirvani, U. Schmidt, S. Kornhuber, and E. Kynast, "Proposal for a general atmospheric correction method of breakdown and withstand voltages of air-gap insulated configurations based on a streamer-leader differentiated model of the breakdown process," Energies, vol. 11, no. 4, 2018,

[15] D. Schlesinger, "Organizational culture," 2017 Jt. Rail Conf. JRC 2017, 2017

[16] C. T. 0. SC33, "Humidity influence on non-uniform field breakdown in air," Electra, vol. 134. pp. 62–89, 1992.

[17] L. Omkristallisation, "Laboration 1. Omkristallisation," pp. 3–5.

[18] A. H. Mostajabi, M. H. Samimi, M. Arabzadeh, A. A. S. Akmal, and H. Mohseni, "EFFECT OF HUMIDITY ON THE BREAKDOWN VOLTAGE OF INSULATORS AT VARYING HUMIDITY AND TEMPERATURE CONDITIONS."

[19] P. N. Mikropoulos, C. A. Stassinopoulos, P. N. Mikropoulos, and C. J. Bagavos, "Positive impulse humidity correction factor for medium rod-plane gaps Soil ionization View project Stochastic (fractal-based) simulation modeling for lightning protection studies View project POSITIVE IMPULSE HUMIDITY CORRECTION FACTOR FOR MEDIUM ROD-PI'ANE GAPS," 1992.

[20] M. M. Ispirli, Ö. Kalenderli, F. Seifert, M. Rock, and B. Oral, "The Effect of DC Voltage Pre-Stress on the Breakdown Voltage of Air under Composite DC and LI Voltage and Test Circuit: Design and Application," Energies, vol. 15, no. 4, 2022,

[21] ISO 25178-2:2012, International Standard International Standard, vol. 2003. 2003.

[22] ICE31010, "International Standard International Standard," 61010-1 © Iec2019, vol. 2019, p. 268, 2019.

[23] J. Hällström et al., "Applicability of Different Implementations of K-factor Filtering Schemes for the Revision of IEC60060-1 and -2," 2005.

[24] J. Hu et al., "Positive switching impulse discharge performance and voltage correction of 1-m rod-plane air gap," IEEE Trans. Power Deliv., vol. 22, no. 2, pp. 1247–1254, 2007

[25] https://en.wikipedia.org/wiki/Machine learning

[26] D. E. Gourgoulis, P. N. Mikropoulos, and C. A. Stassinopoulos, "On the breakdown parameters of medium length rod - plane gaps stressed by positive impulse voltages with long wavetails," Proc. Univ. Power Eng. Conf., vol. 3, no. July, pp. 744–747, 1996.

[27] A. Fischer, "The influence of humidity on DC and AC breakdown voltage of air gaps," Electra, vol. 10. pp. 65–77.

[28] K. Feser and A. Pigini, "Influence of atmospheric conditions on the dielectric strength of external insulation 112.pdf," Electra, vol. 112. pp. 83–95, 1987.

[29] K. Feser, "Influence of Humidity on the Breakdown Voltage of DC and AC Voltages in Air," Bull. ASE, vol. 63, no. 6, pp. 278–281, 1972.

[30] M. A. Fard, M. E. Farrag, A. Reid, and F. Al-Naemi, "Electrical treeing in power cable insulation under harmonics superimposed on unfiltered HVDC voltages," Energies, vol. 12, no. 16, 2019

[31] M. A. Fard, M. E. Farrag, S. McMeekin, and A. Reid, "Electrical treeing in cable insulation under different HVDC operational conditions," Energies, vol. 11, no. 9, pp. 1–14, 2018

[32] C. De Salles, J. P. Pennacchi, and M. L. B. Martinez, "A new proposal to determine the humidity correction factor for Lightning Impulse Tests and application to commercial configurations," in 2003 IEEE Bologna PowerTech - Conference Proceedings, 2003, vol. 2, pp. 828–831.

[33] P. A. Calva Chavarria and A. Robledo-Martinez, "Effect of humidity on DC breakdown voltages in ambient air at high altitude," Conf. Electr. Insul. Dielectr. Phenom. (CEIDP), Annu. Rep., vol. 2, pp. 567–570, 1996

[34] W. Buesch, "Air Humidity: an Important Factor for Uhv Design.," no. 6, pp. 2086–2093, 1978.

[35] S. Berlijn et al., "Today's problems with the evaluation methods of full lightning impulse parameters as described in IEC 60060-1," IEE Conf. Publ., vol. 1, no. 467, 1999

[36] D. Ariza, A. Beroual, R. Methling, S. Gortschakow, and H. R. Chamorro, “First-mode of negative streamers: Inception at liquid/solid interfaces,” High Volt., vol. 6, no. 6, pp. 1069–1078, Dec. 2021

[37] D. Ariza, A. Beroual, R. Methling, S. Gortschakow, and H. R. Chamorro, “First-mode of negative streamers: Inception at liquid/solid interfaces,” High Volt., vol. 6, no. 6, pp. 1069–1078, 2021

[38] L. Arevalo, D. Wu, and M. Larsson, “Air humidity factor for external insulation under positive switching impulses - Revisited,” Lect. Notes Electr. Eng., vol. 599 LNEE, pp. 784–794, 2020

[39] https://matlabacademy.mathworks.com

[40] https://www.techtarget.com/searchenterpriseai/definition/machine-learning-ML

[41] Rhttps://www.electricaldeck.com/2021/11/what-is-overvoltage-in-power-system.html

[42] ’Modeling of Mathematical Equation for Determining Breakdown Voltage, Laili, Muhammad S and Yusof, Noradila and Zakaria, Zetty N and Razali, Noor A Mohd, 2013 1st International Conference on Artificial Intelligence, Modelling and Simulation, 2013, IEEE

[43] ’MEASUREMENT OF AIR BREAKDOWN VOLTAGE AND ELECTRIC FIELD USING STANDAD SPHERE GAP METHOD’, Sankar2011, Paraselli Bheema Sankar, 2011,

[44] https://corporatefinanceinstitute.com/resources/knowledge/other/r-squared

[45] https://towardsdatascience.com

[46] https://machinelearningmastery.com

[47] https://se.mathworks.com

DEPARTMENT OF ELECTRICAL ENGINEERING

CHALMERS UNIVERSITY OF TECHNOLOGY

Gothenburg, Sweden

www.chalmers.se

CHALMERS

UNIVERSITY OF TECHNOLOGY